DEVELOPMENT OF NON-ADHERENT SINGLE CELL CULTURING AND

ANALYSIS TECHNIQUES ON MICROFLUIDIC DEVICES


by


PERNILLA VIBERG


M.S, Malardalens University, 2003


AN ABSTRACT OF A DISSERTATION


submitted in partial fulfillment of the requirements for the degree


DOCTOR OF PHILOSOPHY


Department of Chemistry
College of Arts and Sciences


KANSAS STATE UNIVERSITY
Manhattan, Kansas


2009

# Abstract

Microfluidic devices have a wide variety of biological applications. My Ph.D. dissertation focuses on three major projects. A) culturing a non-adherent immortal cell line within a microfluidic device under static and dynamic media flow conditions; B) designing and fabricating novel microfluidic devices for electrokinetic injecting analytes from a hydrodynamic fluid; and C) using this novel injection method to lyse single non-adherent cells by applying a high electric field across the cell at a microfluidic channel intersection.

There are several potential advantages to the use of microfluidic devices for the analysis of single cells: First, cells can be handled with care and precision while being transported in the microfluidic channels. Second, cell culturing, handling, and analysis can be integrated together in a single, compact microfluidic device. Third, cell culturing and analysis in microfluidic devices uses only extremely small volumes of culturing media and analysis buffer. In this dissertation a non-adherent immortal cell line was studied under static media flow conditions inside a $CO_2$ incubator and under dynamic media flow conditions in a novel portable cell culture chamber.

To culture cells they must first be trapped on a microfluidic device. To attempt to successfully trap cells, three different types of cellular traps were designed, fabricated and tested in polydimethylsiloxane (PDMS)-based microfluidic devices. In the first generation device, cubic-shaped traps were used. After 48 h of culturing in these devices the cell viability of $79 \pm 6$ % (n = 3). In the second generation device, circular wells with

narrow connecting channels were employed. However, after 12 h of culturing, no viable cells were found. While the second generation device was not capable of successfully culturing cells, it did demonstrate the importance of culturing under dynamic conditions which lead to next design. The third generation microfluidic device consisted of hydrodynamic shaped traps that were used to culture the cells in a less confined environment. The cell viability after 12 h in this design was $29 \pm 41\%$ (n = 3).

In addition to cell trapping, a novel electrokinetic injection method was developed for injecting analytes from a hydrodynamic flow into a separation channel that was followed by an electrokinetic separation. As the hydrodynamic flow could introduce some excess band broadening in the separation, the actual band broadening of an analyte was measured for different channel depths and hydrodynamic fluid flow rates. The results consistently showed that the separations performed on these devices were diffusion limited. Finally, using this novel injection method, single cell lysis was performed by applying a high voltage at the microfluidic channel intersection. The results of these studies may eventually be applied to help answer some fundamental questions in the areas of biochemistry and pharmaceutical science.

DEVELOPMENT OF NON-ADHERENT SINGLE CELL CULTURING AND

ANALYSIS TECHNIQUES ON MICROFLUIDIC DEVICES

by

PERNILLA VIBERG

M.S, Malardalens University, 2003

A DISSERTATION

submitted in partial fulfillment of the requirements for the degree

DOCTOR OF PHILOSOPHY

Department of Chemistry
College of Arts And Sciences

KANSAS STATE UNIVERSITY
Manhattan, Kansas

2009

Approved by:

Major Professor
Christopher T. Culbertson

# Copyright

PERNILLA VIBERG

2009

# Abstract

Microfluidic devices have a wide variety of biological applications. My Ph.D. dissertation focuses on three major projects. A) culturing a non-adherent immortal cell line within a microfluidic device under static and dynamic media flow conditions; B) designing and fabricating novel microfluidic devices for electrokinetic injecting analytes from a hydrodynamic fluid; and C) using this novel injection method to lyse single non-adherent cells by applying a high electric field across the cell at a microfluidic channel intersection.

There are several potential advantages to the use of microfluidic devices for the analysis of single cells: First, cells can be handled with care and precision while being transported in the microfluidic channels. Second, cell culturing, handling, and analysis can be integrated together in a single, compact microfluidic device. Third, cell culturing and analysis in microfluidic devices uses only extremely small volumes of culturing media and analysis buffer. In this dissertation a non-adherent immortal cell line was studied under static media flow conditions inside a $CO_2$ incubator and under dynamic media flow conditions in a novel portable cell culture chamber.

To culture cells they must first be trapped on a microfluidic device. To attempt to successfully trap cells, three different types of cellular traps were designed, fabricated and tested in polydimethylsiloxane (PDMS)-based microfluidic devices. In the first generation device, cubic-shaped traps were used. After 48 h of culturing in these devices the cell viability of $79 \pm 6$ % (n = 3). In the second generation device, circular wells with

narrow connecting channels were employed. However, after 12 h of culturing, no viable cells were found. While the second generation device was not capable of successfully culturing cells, it did demonstrate the importance of culturing under dynamic conditions which lead to next design. The third generation microfluidic device consisted of hydrodynamic shaped traps that were used to culture the cells in a less confined environment. The cell viability after 12 h in this design was $29 \pm 41\%$ (n = 3).

In addition to cell trapping, a novel electrokinetic injection method was developed for injecting analytes from a hydrodynamic flow into a separation channel that was followed by an electrokinetic separation. As the hydrodynamic flow could introduce some excess band broadening in the separation, the actual band broadening of an analyte was measured for different channel depths and hydrodynamic fluid flow rates. The results consistently showed that the separations performed on these devices were diffusion limited. Finally, using this novel injection method, single cell lysis was performed by applying a high voltage at the microfluidic channel intersection. The results of these studies may eventually be applied to help answer some fundamental questions in the areas of biochemistry and pharmaceutical science.

# Table of Contents

# List of Figures

# List of Tables

# Acknowledgements

Dr. Chris Culbertson, Thank you for all your advice and help during these years. Thank you for making me become a better scientist!

Dr. Anne Culbertson, Thank you for all the help in the cell culturing area and for all the helpful advice along the way.

To my committee Dr. John Tomich, Dr. Moiser, Dr. Ito and Dr. Paul Smith, Thank you for your time and helpful comments.

Dr. Greg Roman, Singing or not singing, you are still my AI (American Idol) when it comes to being a researcher.

Dr. Amanda Meyer, than you for being a great co-worker! Thanks for the company during early morning workout sessions and as well as long evenings in the lab.

To the Culbertson group, thank you to all past and current group members. Thank you especially to Kurt, Scott, Jeff, Alex, Kevin, Manuja, Eve and Congkui.

To Susan, Michelle, Myung, Helene, Pinar, Sara, Carolina, Caroline, Jenny, Rebecca and Annika, thank you all for being truly great friends during these years.

To Hjördis Andersson, my high school teacher who started my interest for Chemistry.

Thank you to the K-State Chemistry department. Especially to the helpful staff: Earline, Mary, Brenda, Connie, Donna, Kim, Richard, Jim, Tobe, Ron and Leila.

# Dedication

To my mom and dad, I could not have done this without your love and support through the years. Thank you for always letting me make my own decisions and always believing in me.

To my brother Tobias, Thank you for keeping me grounded and reminding me to see the big picture in life.

To my grandmother Ingrid, Thank you for being a wonderful and truly wise person. You were the first one who taught me about Capillary forces through your cross word puzzles!

To my aunt Siw and uncle Rune, Thank you for all the encouraging emails and support during these years.

To my cousins Camilla and Martiha, You two are like my big sisters. Thank you, to you and your families for all the fun and wonderful advice throughout the years.

To my aunt Rose-Marie and uncle Kent for all the encouraging letters and emails through the years in Kansas.

# CHAPTER 1 - INTRODUCTION

## 1.1 Microfluidics

A goal of modern cell biology is to understand the molecular mechanisms that control cellular functions.[1] Over the past two decades lab-on-a-chip devices have begun to make a significant contribution to the analysis of biological systems.[2] Microfluidic devices offer several potential advantages over traditional cellular analysis techniques, these are introduced below. First, microfluidics allows the precise control and manipulation of small volumes of fluids in channels that have micrometer dimensions. Second, the small dimensions allow for cells to be cultured in an *in vivo* mimicked environment. Third, integration and automation of cell culturing, lysis and separation of the cell lysate is possible. Fourth, the unique combination of a short injection plug of analyte and the high electric fields creates unique conditions for high efficiency separations.[3] Fifth, the substrates from which the devices are fabricated are generally transparent and inexpensive. The transparent nature of the substrate material allows the use of sensitive optical, on-column detection methods such as laser induced fluorescence.

In this dissertation the above properties of microfluidics are taken advantage of and used for cell culturing and the separations of both amino acids and single cell lysates. The eventual aim of the work reported in this dissertation is to develop methods to culture single, non-anchorage dependent cells inside a microfluidic device, then load the cells with a fluorescent protein and perform single cell analyses.

Capillary electrophoresis is a rapid, high separation efficiency, high resolution analytical separation technique which uses small volumes of analyte, buffer and reagents.[4] When this powerful technique is used inside a microfluidic device the benefits are even better. Because of the small dimensions of the microfluidic channels, it is possible to make very low volume injections into the separation channel. The combination of small injection volume picoliter (pL) and high electric field strength results in high efficiency separations. The small micrometer dimensions of the channels also allow for high efficiency, high resolution separations which is important for analyzing complex biological fluids.[5]

## 1.2 Theory

Capillary electrophoresis[6-9] is a powerful separation method that is based upon the differential electrophoretic mobilities of analytes in an electric field. The analytes are separated based on their mass to hydrodynamic radius ratio.[10] By applying an electric field through the channel a potential energy drop is created down the channel. Under such conditions ions migrate at different rates in the electric field as explained below.

### 1.2.1 Transport Mechanisms

The electrophoretic velocity ($v_{ep}$) of charged analytes moving in the channel is dependent on the electrophoretic mobility ($\mu_{ep}$) of the analyte and the electric field strength ($E$) applied along the capillary as shown in E1.1.

$$v_{ep} = \mu_{ep}E \qquad\qquad (E1.1)$$

There are two forces on the analyte in the separation channel, an electrical force and a frictional force. The electrical force ($F_E$) is dependent on the charge ($q$) of the analyte and the electric field ($E$) that is being applied (E1.2).

$$F_E = qE \qquad\qquad\qquad (E1.2)$$

The frictional force ($F_F$) (E1.3) is directed in the opposite direction of the electrical force. This force depends on the viscosity of the media in which the separation takes place ($\eta$), the hydrodynamic radius of the analyte ($r$) and the electrophoretic velocity ($v_{ep}$) of the analyte. This equation is commonly known as Stoke's law[11].

$$F_F = -6\pi\eta r\, v_{ep} \qquad\qquad\qquad (E1.3)$$

In electrophoresis, there is a steady state in which these two forces are at equilibrium, but in opposite directions. By combining the three equations above, we find that the electrophoretic velocity depends upon the charge of the analyte, electric field strength, hydrodynamic radius of the analyte, and the viscosity of the media (E1.4).

$$v_{ep} = \frac{qE}{6\pi\eta r} \qquad\qquad\qquad (E1.4)$$

Under a given set of separation conditions $q/6\pi\eta r$ is constant and called the electrophoretic mobility ($\mu_{ep}$). The analyte with the highest electrophoretic mobility, i.e. a large positive charge and a small hydrodynamic radius will migrate the fastest toward the cathode. Neutral analytes feel no net force and anions are attracted to the anode.

### 1.2.2 Electroosmic Flow (EOF)

Electroosmotic flow[12] is a form of fluid transport that takes place in small diameter ionic-buffer filled capillaries when an electrical potential is applied axially

along the channel.  Electroosmosis generates bulk transport of the fluid in the capillary

channel. The inside of a glass or fused silica microfluidic channel has a negative charge

at pH values over 3. The negative charges on the wall are generated by ionized silanol

groups and attract cations from solution to neutralize the charge.  These cations will form

an electrical double layer near the surface. The first layer of this so-called double layer

consists of ions that adsorb strongly to the wall and partially dehydrate. This layer is

called the Stern layer. Because the adsorbed ions do not completely neutralize the charge,

a second more diffuse layer of hydrated cations forms. This layer begins at what is called

the Outer Helmholz Plane (OHP). The diffuse layer extends from the outer Helmholtz

plane to the bulk solution where charge neutrality prevails. The thickness of this layer is

dependent upon the concentration of ions in solution, but under typical buffer conditions

for electrophoresis the layer is <30 nm thick. It is the diffuse layer that determines the

zeta potential ($\zeta$) and the velocity of the electroosmotic flow ($v_{eo}$). The velocity of the

bulk fluid in a capillary channel due to the electroosmotic flow ($v_{eo}$) can be described

using equation E1.5

$$v_{eo} = \frac{k\varepsilon_0 \zeta \mathrm{E}}{\eta} \qquad\qquad \text{(E1.5)}$$

where k is the dielectric constant, $\varepsilon_0$ is the permittivity if free space, $\zeta$ is the zeta

potential of the channel wall, $\eta$ is the viscosity of the buffer solution and $E$ is the applied

electric field strength.


The hydrated cations in the bulk solution move the flow toward the cathode,

because as ions is transported from positive (high voltage) toward negative (ground), they

drag water molecules along with their sphere of hydration. These water molecules in turn

drag along with other water molecules resulting in a bulk solution flow toward the

cathode. The EOF does not separate the analytes, it merely sweeps them through the

channel toward the cathode. Generally the magnitude of the EOF is greater than the

electrophoretic velocity of the anions and so both cations and anions migrate toward the

cathode. Neutral molecules will travel at the EOF velocity. Another important advantage

of EOF is that the fluid flow profile is flat (Fig. 1.1B), meaning that the velocity across

the capillary diameter is similar at the wall and in the middle of the channel. However it

is important to note that the analyte velocity within a few nm of the wall is close to zero.

### *1.2.3 Parabolic Flow*

When a pressure driven flow is used to move fluids, the fluid flow profile in the

channel will be parabolic in shape. This fluid flow profile is generated by the resistance

to flow at the channel wall. The fluid flow resistance is highest at the channel wall, which

is shown in Fig 1.1A by the smallest arrows. However for fluid elements closer to the

middle of the capillary, the effect of the resistance will be smaller and smaller and,

because of this, the overall velocity of the fluid is going to be highest in the middle of the

channel. The overall velocity ($v$) of the fluid flow in a capillary under pressure induced

flow conditions  can be related to the channel volumetric flow rate ($F_c$) and the channel

cross section ($A_c$) as shown in E1.6.

$$v = \frac{F_c}{A_c}$$
(E1.6)
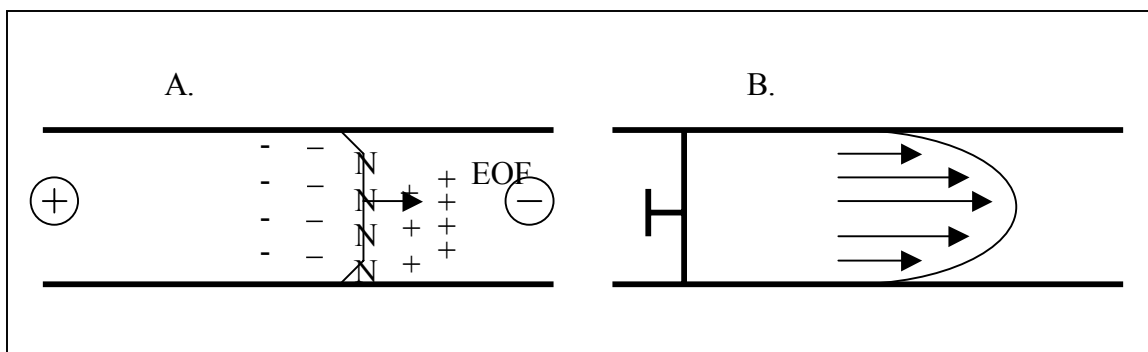
**Figure 1.1 - An illustration of Electroosmotic flow (A) and Hydrodynamic flow (B) in microfluidic channels.**

Parabolic fluid flow is detrimental to separations because it leads to band broadening, as will be discussed in Chapter 4.

### *1.2.4 Band Broadening*

After the analyte plug has been injected into the separation channel there are several factors that lead to broadening of the injection plug. These include diffusion, injection, detection, parabolic flow Joule heating, electrodispersion, channel geometry, and mass transfer. Band broadening due to longitudinal diffusion ($\sigma_{diff}$) will always be present. This broadening of the peak can be expressed by the Einstein-Smoluchowski equation. The longitudinal diffusion ($\sigma^2_{Diff}$) is dependent on the diffusion coefficient ($D$) of the analyte and the separation time ($t$).[13] This relationship is shown in E1.7.

$$\sigma^2_{Diff} = 2Dt \qquad \text{(E1.7)}$$

The second source of band broadening is the injection plug length ($\sigma^2_{inj}$) in the separation channel. It is dependent on the injection length[14] ($l_{inj}$) as shown in E1.8.

$$\sigma^2_{inj} = \frac{l_{inj}^2}{12} \qquad \text{(E1.8)}$$

The third source of broadening is due to the size of the detection window. For separation using laser induced fluorescence (LIF) the detection window is generally defined either by the laser spot size in the capillary or the spatial filter in front of the detector. Band broadening due to detection is generally small in comparison to longitudinal diffusion. The band broadening due to the detection window ($\sigma^2_{det}$) is dependent on the detection window length ($l_{det}$) as shown in E1.9. This contribution is constant and for LIF detection with effective projected detection window apertures < 20 μm, the band broadening due to the detection window is insignificant and can be ignored.[15]

$$\sigma^2_{\text{det}} = \frac{l^2_{\text{det}}}{12} \qquad\qquad \text{(E1.9)}$$

The fourth source of band broadening is due to parabolic fluid flow. This can be generated from Joule heating or a hydrodynamically generated flow such as that from a pump or unlevel reservoirs. The band broadening due to the parabolic flow is dependent on the fluid velocity ($v_{para}$), channel depth ($d$), diffusion coefficient of the analyte ($D$) and the separation time ($t$) according to E1.10. This factor will be further discussed in chapter 5.

$$\sigma^2_{para} = \frac{4}{105}\frac{v^2_{para}d^2t}{D} \qquad\qquad \text{(E1.10)}$$

Additional band broadening factors such as joule heating, mass transfer, geometric factors and electrodispersion can also occur but they can generally be eliminated or minimized for most electrophoretic separations. Joule heating refers to electrical energy being converted into heat energy inside the capillary which can alter the viscosity of the fluid which leads to band broadening.[16] Mass transfer can be eliminated

since no stationary phase is used in the microfluidic channels.[17] Geometric dispersion is generated when there are turns on the separation channel before the detection point and can be eliminated because of no such patterns are used.[18] Electrodispersion is generated when there is a significant difference in conductivity of the analyte band and the background buffer. This effect can be minimized by diluting the sample in the background buffer and using a sample concentration of 400-1000-fold less than the buffer solution.[19]

Separation efficiency is a common means of reporting on the quality of separations. Under optimized conditions most of the band broadening factors discussed above will be minimized and only the longitudinal diffusion will remain. The separation efficiency ($N$) is determined by the length over which a separation ($l$) is generated squared over the band broadening due to diffusion ($\sigma^2$) according to E1.11

$$N = \frac{l^2}{\sigma^2}$$
(E1.11)

The length of the separation is related to the overall velocity of the analyte ($v$) and separation time ($t$) as shown in E1.12

$l = vt$ (E1.12)

The electrokinetic velocity ($v_{ek}$) is calculated from the electrokinetic mobility ($\mu_{ek}$) and the electric field strength ($E$) shown here

$v_{ek} = \mu_{ek}E$ (E1.13)

By combining the three equations above and E.1.7 it can be shown that the separation efficiency is dependent on the mobility ($\mu_{ek}$), electric field strength ($E$), separation length ($l$) and the diffusion coefficient for the analyte ($D$) according to equation E1.14.

$$N = \frac{\mu E l}{2D}$$ (E1.14)

A second way to determine the quality of a separation is resolution which measures the separation systems ability to separate two analyte bands. The resolution is a function of the difference in migration times of the two analyte bands and the band widths ($\sigma$) of the two analytes denoted 1 and 2 according to equation E1.15.

$$R = \frac{t_2 - t_1}{2\sigma_1 + 2\sigma_2}$$ (E1.15)

The relationship between the separation efficiency and resolution can be expressed by the Purnell equation in E1.16. The resolution is dependent on the separation efficiency ($N$), selectivity ($\alpha$) and the capacity factor ($k_2$).

$$Rs = \frac{N^{1/2}}{4} \left( \frac{\alpha - 1}{\alpha} \right) \left( \frac{k_2 + 1}{k_2} \right)$$ (E.1.16)

## 1.3 Fabrication of Microfluidic Devices

Microfluidic devices can be fabricated from many different materials such as glass, ceramics, polymers and silicon elastomers.[20] In the experiments reported below in this dissertation two types of materials were used, White Crown glass and poly(dimethylsiloxane) (PDMS). Each of these materials has several advantages and disadvantages. Starting with the microfluidic devices made from glass, the advantages are that glass devices can be used with high electric field strengths which are important for high efficiency separations. The surface of the channels in these devices is hydrophilic and has a good solvent resistance. On the other hand, many groups have reported that fabrication methods are difficult, but our group has developed a simple, straightforward

method which does not require a clean room facility. PDMS has the advantage of being an inexpensive elastomeric material. The fabrication of PDMS-based microfluidic devices is rapid and straightforward and does not require a clean room facility. PDMS is the biocompatible and gas permeable. These advantages of PDMS will be discussed further in Chapter 3. A disadvantage of using PDMS as a substrate is that the channel surface are hydrophobic which can lead to the adsorption of analytes and difficulties in filling the channels with hydrophilic solvents. Two methods will be discussed in Chapter 3 to create a hydrophilic PDMS surfaces.

### *1.3.1 Glass Microfluidic Devices*

Glass microfluidic devices can be fabricated using standard lithographic and wet etching processes.  All three types of glass - Soda Lime, Borosilicate and White Crown - used to fabricate the microfluidic devices reported in this dissertation follow the same general protocol outlined below. . The process starts with creating the desired channel design. This pattern was drawn in-house using AutoCAD LT 2002 program from Thompson Learning (Albany NY). The AutoCAD design was sent electronically to Photoplot Store in Colorado Springs, CO for translation and fabrication. The photomask was placed on top of a glass plate (4 x 4") coated with a chrome and AZT positive tone photoresist (Telic Co. Santa Monica, CA). The plate was then exposed to UV-light for 5.00 s using a flood exposure system (ThermoOriel, Stratford, CT). To develop the pattern, the plate was submerged in a Microposit Developer (Shipley Co., Marlborough MA) for 1 min and 30 s followed by carefully rinsing with distilled-deionized water (Barnstead E-pure System, Dubuque,IW). The plate was then submerged in a solution of Chrome Mask Etchant (Transene, Co., Danvers MA) for 3 min and again rinsed with the

10

deionized distilled water. The microfluidic channels were wet etched with by submerging the plate in a dilute solution of buffered oxide etchant ($NH_4F/HF$, 10:1), double-distilled water and hydrochloric acid in a ratio of 1:4:2. The etching rate was approximately 1 μm/min and the etching time was altered depending on the desired channel depth. Each microchip was checked for the proper channel dimensions using a stylus-based Profiler (Ambios Technology Santa Cruz, CA). After the appropriate depth had been reached the plate was removed from the etching solution and rinsed with double distilled water. The remaining photoresist was removed by rinsing the plate with acetone and then double distilled water before submerging in the Chrome Mask Etchant for 10 min followed by a rinse with double-distilled water. The channel plate was then diced into 8, 1" x 2" slides using a MTI Corp dicing saw (Richmond, CA). A bottom plate for each channel plate was fabricated with the second glass plate that was diced into the same dimensions as the channel plates. During the dicing, the plate was adhered to a back plate using wax to hold the glass slides in place while sawing. After dicing, the individual glass slides were submerged into hexanes to dissolve the wax. Reservoirs were drilled into the channel plate using a Dremel Multipro tool (Model 395, Racine WI) with a RioGrande mini diamond drill (2 mm diameter).

The glass slides, top plates and channel plates, were thoroughly cleaned using chemical swabs with hexanes, followed by acetone and then ethanol. The slides were then finally rinsed with double-distilled water and dried with a gentle flow of Argon gas. To clean the surface further, the glass slides were submerged into 5 M sulfuric acid for 10 min and rinsed with double distilled water again and dried with the Argon gas. The entire process, except for the sulfuric acid step was repeated. The glass slides were collected in

a small basket that held the individual glass slides separated in a parallel lineup in the laminar flow hood (Labconco, Kansas City, MO). The basket was submerged in a VersaClean soap solution and sonicated (Branson, Dabury, CT) for 15 min, rinsed with double distilled water and dried with the Argon gas. Then the glass plates were submerged into a solution of acetone and sonicated for 10 min, followed by drying with Argon gas. The basket was then submerged in the dilute buffer oxide etch for 20 s and then placed in a

60 °C hydrolysis solution containing $NH_4OH$, $H_2O_2$, $H_2O$ in the ratio 1:1:2 for 15 min. The slides were rinsed with double distilled water and sonicated under a continuous rinse of double distilled water before being joined together. To bond the glass slides together, the channel plate was taken out first under a continuous stream of double distilled water and placed on a Clean room Wiper (DURX 670: Great Barrington MA), then the bottom plate was taken up under the same conditions and by firmly holding the two glass slides 1 cm apart between the thumb and the index finger, the slides were rinsed with double distilled water. After the glass slides were rinsed with double distilled water for 5-10 s, they were joined together and held with binder clips to create an even pressure over the device, to push out the water between the plates. The glass devices were dried off by a steady flow of Argon gas and the channels were dried out by vacuum. The device was then placed in a 95 °C oven (Fisher Scientific, Pittsburgh, PA) for 30 min to evaporate any remaining water. The devices were then thermally annealed in an oven (Evenheat Kiln Ind oven, Caseville, MI) where the temperature was gradually ramped to 565 °C to ensure irreversible bonding between the channel plate and the bottom plate. Glass reservoirs were glued around the drilled holes in the channel plate using Epo-tek

353ND Epoxy (Epoxy Technologies, Inc., Billerica, MA) in a mixture of Part A to Part B in the ratio 10:1.

### 1.3.2 Poly(dimethylsiloxane)(PDMS) Microfluidic Device

The master mold fabrication[21] was straightforward and fast. Once a master mold was fabricated, a PDMS device could be made in less than one hr. The procedure started by cleaning a glass slide (Corning Glass slide 2" x 3" (2947-75x50) by applying a steady stream of Argon gas over the entire surface. The glass slide was then placed in the holder of a spin coater (Spin coater, Laurell Technology Corporation, Mocel WS-400A-6 NPP/LITE). Negative photoresist (SU-8 2035 MicroChem Corp, Newton MA) was applied evenly over the entire surface. Photoresists are made of a polymer, photosensitizer and casting solvent. A negative photoresist is crosslinked upon exposure to light to make it insoluble in the developing solution. The negative photoresist was exposed to UV-light for 5 s from a flood exposure system (ThermoOriel, Stratford, CT) through a photomask. Areas of the photoresist which have not been exposed to UV-light, can be dissolved away by the developing solution. After exposure, the photoresist was post-baked on a hot plate (Fisher Scientific hotplates). The photoresist pattern was developed in a SU-8 developer (Microposit 351 Developer, MicroChem Corp, Newton MA) for 1 min and then rinsed with isopropanol. Finally the pattern was dried under a careful flow of Argon gas. The raised photoresist pattern which remained was used as the master mold for the PDMS cell culture devices. The exact protocol can be found in Appendix 2. The entire process is shown in Fig 1.2.
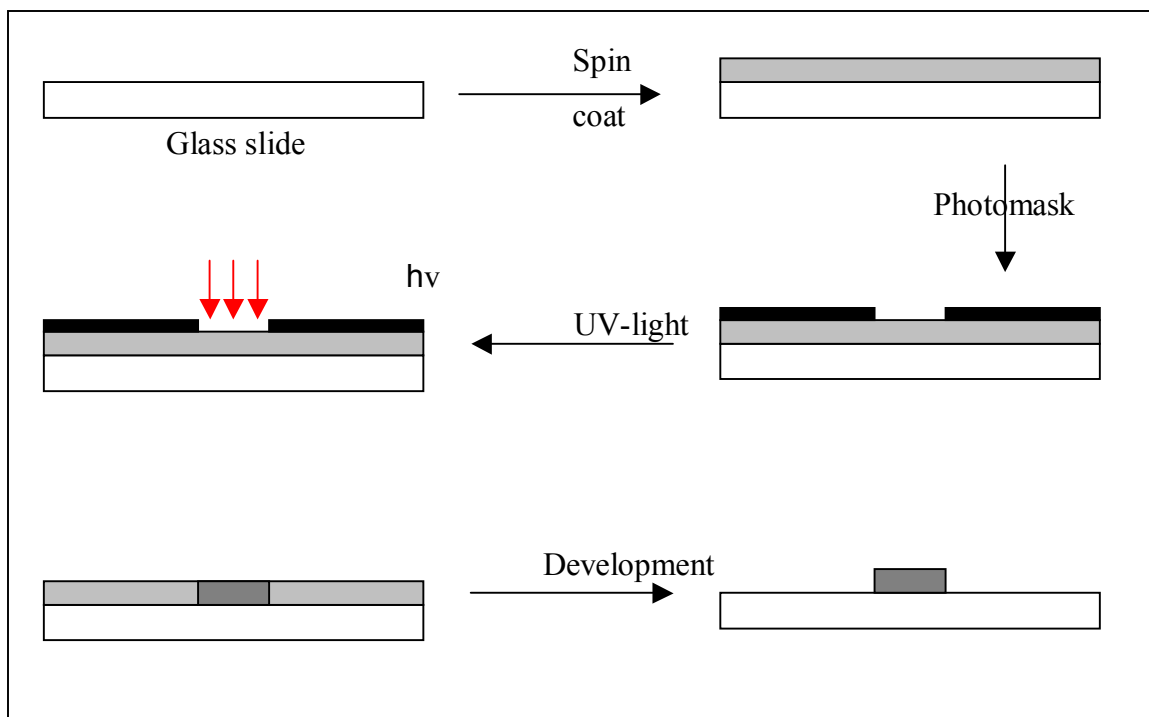
**Figure 1.2 - The photolithography fabrication process for a master mold.**

A new polymer device can be fabricated in less than one hr once the mold in made. In order to fabricate such a device, poly(dimethylsiloxane) (Sylgard®184 Dow Corning, Midland MI) was mixed with the elastomer curing agent in the ratio 10:1. The mixture was hand stirred continuously for two min, then placed in a vacuum dessicator for 30 min to remove excess air. After degassing the polymer was poured carefully onto the master mold with the desired channel design inside the 80°C oven (Lindberg/ Blue Mechanical Convection Ovens). The polymer was then cured for 30 min. The polymer device was then carefully removed from the master mold using a new razor blade and cutting around the device. Once all the edges were loose, the device was carefully removed from the substrate in a diagonal motion. Reservoirs were made into the PDMS channels using a biopuncher (Premier, Plymouth Meeting, PA) to create an opening for

the fluid flow going in and out. It is easier to make the holes before the two PDMS devices are cured together. The channel plate was then aligned with bottom PDMS device and gently the two surfaces where joined together. The device was placed in the 80°C oven for further curing of the polymer for 30 min. PDMS channels are hydrophobic which makes them difficult to fill. Several methods will be discussed in Chapter 3 to make the surface more hydrophilic.

## 1.4 Analysis Methods

### *1.4.1 Single Point Detection Setup*

In order to detect fluorescent analytes at specific distances in a separation channel, a laser must be narrowly focused into the channel and the light emitted by the analytes as they pass through the laser beam must be detected. This detection is performed using what is typically called a single point detection setup. The single-point setup utilizes a 488 nm plasma line of an Argon ion laser excitation source (Melles Griot Laser group, Carlsbad, CA) (shown in Fig. 1.3). In this setup, the light from the laser is sent into a dichroic mirror (Omega Optical, Brattleboro, VT) and then focused through a 20x objective lens (Nikon Instrument Inc, Melville NY) to reach the microfluidic separation channel where the fluorescently labeled analyte was excited by the laser beam. When the fluorophore relaxes back to ground state light is emitted. The light is collected using a the same microscope objective used for excitation, passes back through the dichroic mirror and then is reflected by a mirror (Thorlabs Inc, Newton NJ). The light passes through a spatial (800μm) filter (Omega Optical, Brattleboro, VT) and a spectral filter (Omega Optical, Brattleboro, VT), then through a notch filter (Kaiser Optical

Systems Inc, Ann Arbor MI ) and finally is detected at the photomultiplier Tube (PMT) (Research Inc, Danvers, MA). The signal is amplified by a low noise current pre-amplifier (Stanford research systems, Sunnyvale, CA) and sent to a computer using LabVIEW™ data acquisition hardware. Data acquisition was controlled through an in-house written LabView 8 program. The high voltages electrodes were also controlled using the same LabView card (National Instrument SCB-68, 6036E card) and data acquisition program. This technique allows for injection times on microfluidic devices as short as 20 ms.
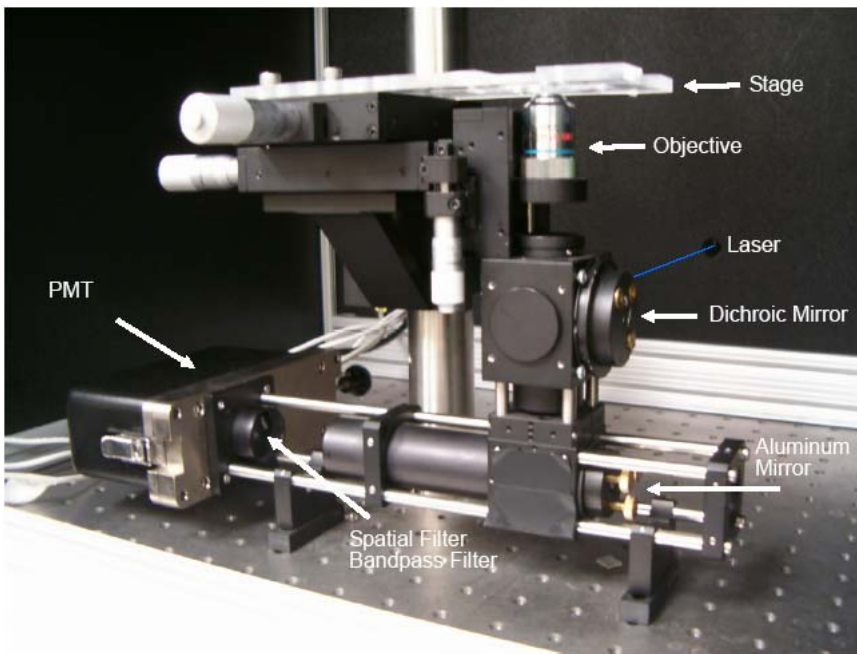


**Figure 1.3 - The Single point setup used for separations of fluids, particles and cells.**

### *1.4.2 Analyte Detection with Laser Induced Fluorescence (LIF)*

In order to detect the analytes used for the experiments in this dissertation they had to be chemically derivatized with fluorescent probes. The limit of detection for such probe is generally in the picomolar range. Previously, detecting intracellular proteins from a single cell has been challenging due to their extremely low concentration, but this

16

can be done using laser induced fluorescence. With the help of a fluorescent tag such as fluorescein-5-isothiocyanate (FITC)[22] analytes at low nanomolar concentrations can be detected using LIF. This is a powerful technique yielding high sensitivity and selectivity.

### 1.4.3 Fluorescent Tags used for Detection of Amino Acids

The fluorescent tags used to label the amino acids used in these experiments were fluorescein-5-isothiocyanate (FITC) (Fig 1.4). The dye were purchased from Invitrogen, Carlsbad, CA and used without further purification. The FITC has a molecular weight of 389.38 g/mol. There are several ways to attach a fluorophore to the analyte, the most common involve a bond formation with amines, thiols or alcohols.[23]
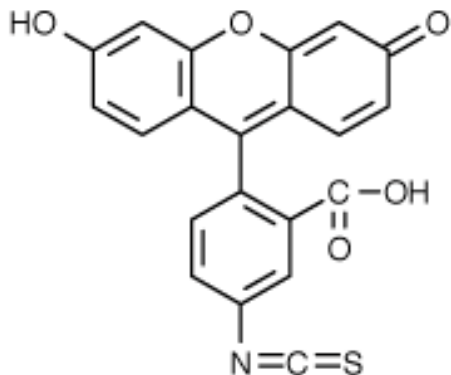


**Figure 1.4 - Structure of Fluorescein-5-isothiocyanate (FITC).[22]**

The FITC molecule has an excitation range between 480-490 nm and an emission spectra range between 525-545 nm, as shown in Fig 1.5.
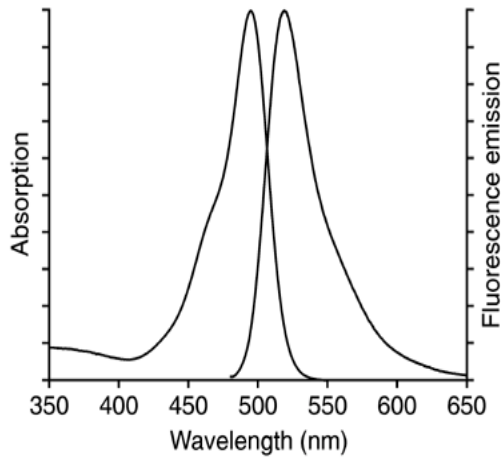
**Figure 1.5 - The excitation and emission spectra of Fluorescein-5-isothiocyanate (FITC).[22]**

### *1.4.4 Calculating Specific Flow Resistances*

The flow rate ($Q$) in microfluidic channels is proportional to the change in pressure ($\Delta P$) and inversely proportional to the resistance ($R$) of the fluid flow according to E1.17:

$$Q = \frac{\Delta P}{R} \qquad \text{(E1.17)}$$

This approximation can be used for fluidic calculations such a those for hydrodynamic fluidic flows. The resistance in the microfluidic channel can be calculated from the fluid viscosity ($\mu$), channel length ($L$) and the radius of the capillary ($r$) as seen in E.18

$$R = \frac{8\mu L}{\pi r^4} \qquad \text{(E1.18)}$$

By combining the resistance from equation E.1.17 and E1.18, the flow rate can be expressed as:

18

$$Q = \frac{\Delta P \pi r^4}{8\mu L} \qquad \text{(E1.19)}$$

These equations are based on circular channels, however the glass channels used for these separations are nearly rectangular, because of the isotopic etching. The average flow rate in a rectangular channel is described in E1.20[24] where $w$ is the half width, $d$ is the half depth ($d$), and F is the form factor:

$$Q = \frac{wd}{\mu} \frac{\Delta P}{L} F \qquad \text{(E1.20)}$$

Rearrangements of the equation yield E.1.21, where A is the cross section area is:

$$\Delta P = \frac{\mu L Q}{wdF} = Q \frac{4}{A} \frac{\mu L}{F} \qquad \text{(E1.21)}$$

Equation E.1.21 can be rewritten into E1.22:

$$\Delta P = \frac{Q}{A}\left(\frac{\mu L}{wdF}\right) = Q\left(\frac{4\mu L}{(wd)^2 F}\right) \qquad \text{(E1.22)}$$

The fluid flow calculations are significant for the microfluidic devices (Fig 1.6) used for separations in Chapter 5. In the experiments described in Chapter 5 there is a need to balance the parabolic flow caused by a syringe pump and the electrokinetic flow at the microchip channel intersection. The parabolic flow rates used ranged 50-300 nL/min, as flow rate is increased it could lead to excess band broadening of the analyte plug as it migrates down the separation channel. In the design below the fluid flow resistance difference is approximately 50 times higher in the separation channel than in the other channels. This high fluidic resistance in the separation channel minimizes the

back flow of fluid from this channel, into the lower right reservoir which was connected

to a syringe pump. This will be discussed further in Chapter 5.
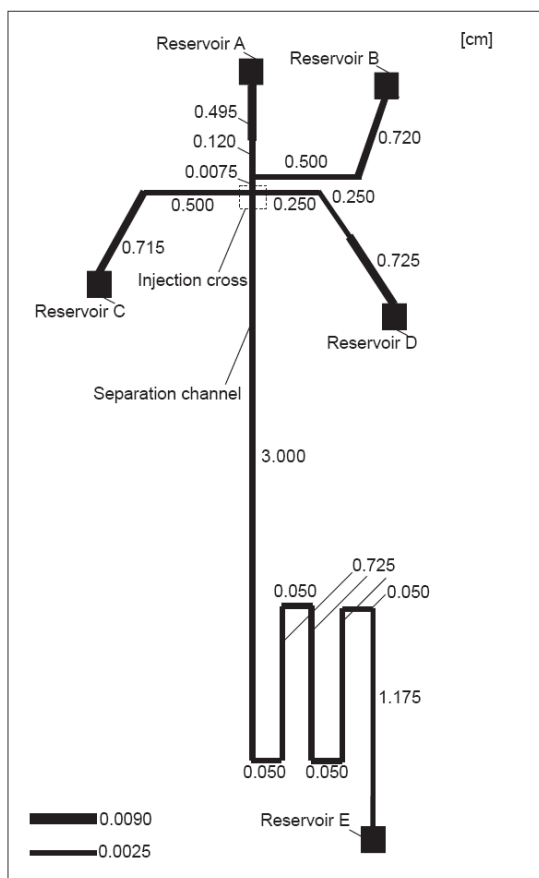
**Figure 1.6 - An image of the microfluidic channel design for amino acid separations.**

# CHAPTER 2 - REVIEW OF PREVIOUS CELL CULTURE AND SINGLE CELL ANALYSIS

## 2.1 Introduction

The background information in this chapter should serve as an introduction to the experiments and results reported in chapters 3-5.

### *2.1.1 Traditional Cell Culturing*

The earliest attempts at cell preservation were made in the late 19th century when mammalian bull spermatozoa cells were frozen and saved for an extended period of time and then recovered for artificial insemination. These cells were used for selective breeding of cattle. The first tissue culture experiment was reported by Ross Harrison in 1907[25]. *In vitro* culturing is advantageous because of the ability to control the local environment of the cells. Parameters such as temperature, pH, osmolarity, dissolved gases; and the addition of additives such as nutrients and hormones can be controlled.[26, 27] An additional benefit is that cell culture can partially replace the need for animal experimentation. There are, however, limitations to cell culturing. For example, the cells need to be cultured under sterile environment to prevent contamination of the culture by bacteria or other microbes. Handling with these samples requires expertise from trained personal. In order to produce large quantities of "homogenous" cells for experiments

21

roller bottles, cell culture flasks, and Petri dishes are used. These containers require approximately 10-25 mL of media. The ability to culture cells on a small scale on microfluidic devices would save time and money. Microfluidic cell culturing devices could also be used as a platform to study cell growth and division over extended periods of time without exposing the cell to potential contamination through passaging. In this chapter the potential for cell culturing inside a microfluidic device is explored.

### 2.1.2 The Cell, an Unique Sample

A typical eukaryotic cell (Fig. 2.1) has a diameter of 10-100 μm, a volume of 0.1-8.0 picoliter (pL), potentially containing over 10,000 different compounds[28] and approximately 100,000 different proteins.[29-31] The ability to analyze single cells is essential for fundamental understanding of the cell for numerous reasons as listed below. First, the individual cells have discrete molecular, metabolic and proteomic identities which interconnect with other cells.[32] In order to understand these interactions and the chemical released individual cells need to be studied. Second, there can be significant variations in responses from individual identical cells, meaning cells originating from the same cell line, same passage number and the same flask respond differently to external factors.[33-35] Factors that influence the cell response can be soluble chemicals and gases, cell to cell interactions, cell substrate interactions, mechanical forces applied on the cell, and the thermal environment. These stimuli can result in a change in the cellular functions and/or changes in gene expression.[36-41] This phenomena is due to the variations of protein expression throughout the cell cycle.[33, 36-41] The causes for these differences are temporal and spatial stochasticity in the chemical processes in the individual cell. Third, cells studied by bulk methods only give average values for analyte concentrations.[35]

Fourth, single cell studies of tumors biopsies have shown that the majority of cells within the tumor may be normal and that there is considerable heterogeneity among abnormal cell.[42, 43] Fifth, many biological studies require data from a large population (> 1000) of cells. But key biological states, such as stem cells occur in low numbers of cells, whose information is lost in bulk measuring methods.[44] Sixth, in a resent proteomics study[45] 1000 different endogenously tagged protein in a human cancer cell were investigated while responding to a chemotherapy drug. These types of studies will broaden our understanding of molecular response to drugs in individual cells which is of significant interest to the pharmaceutical research.
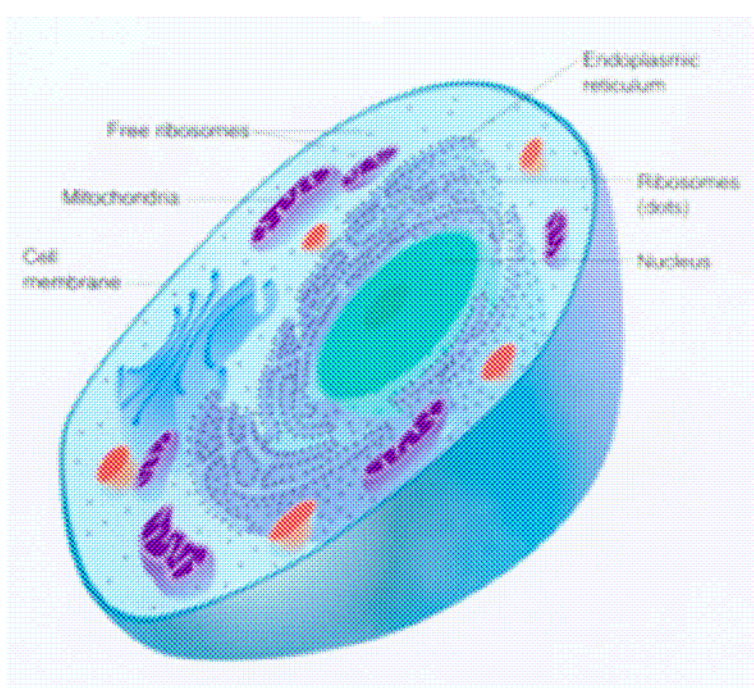


**Figure 2.1 - A mammalian cell.[31]**

Cultured cells can be divided into two major categories, anchorage dependent and non-anchorage dependent cells.[25, 27] As the names imply, the first are a group of cells that require attachment to a substrate to form a monolayer of cells. The anchorage dependent cells are the most common cells, since the majority of cells from solid tissue. The second

23

group, non-anchorage dependent cells also called suspension cells, these cells can move freely in solution without being attached to a substrate. Culturing anchorage dependent cells in microfluidic devices does have the advantage that the cells stay in place during culturing. In these experiments only suspension cells are used since the fundamental idea of the device is to transfer cells from the cell culturing area to be labeled and finally to be analyzed with as little interference to the cell as possible.

If anchorage dependent cells are used for these experiments, the cells must be mobilized by chemicals such as Trypsin-EDTA. The disadvantage is that during the detachment process unwanted cell signaling reactions can be initiated. This may interfere with the cell signaling within the cell, since many cell signaling events takes less than 1 s. For example, metabolite concentrations can change 10-fold in 1 s and enzymes have a usual turnover number on the order of $1x10^{-4}$ s.[46] Our goal is to handle cells with minimal interference prior to analysis.

## *2.1.3 Cancerous Cells*

The major difference between a normal cell and a cancer cell is that the latter has lost the control of several important cellular functions, which leads to an increase in cell division. Normal cells are mortal, meaning that these cells have a limited number of divisions and then die. Cancer cells can be immortal and continue to grow almost indefinitely. Normal cells generally exhibit contact inhibition. Meaning that the cell density reaches a limit and the cell growth is reduced. Cancerous cells do not have this feature, which makes cancer cells grow to form overlapping layers or tumors. The third major issue is that normal cells are dependent on growth factors, where cancer cells are less dependent on growth factors[25].

## *2.1.4 Advantages of Culturing in Microfluidic Devices*

The general advantages of microfluidics are: 1) the small size of the channels in the device allow high efficiency separations to be performed, 2) only small volumes of analyte and expensive reagents are needed, and 3) the ability for chemical analyses to be integrated and automated.[5] The specific advantages that make microfluidic technology suitable for single cell analyses are given below. First, cells can be handled with care and precision while being transported in the microfluidic channels because the channels are only slightly larger than the cell themselves. Second, cells can be directly cultured on the microfluidic devices. Third, integration of the cell handling and analysis processes are possible. This includes the integration of cell culturing, lysis, injection of lysate into the separation channel, and separation of the cell lysate onto a single monolithic device. Fourth, a gated injection can produce a short injection plug, which in combination with a high electric field strength, creates unique conditions for high efficiency separations. Fifth, the microfluidic substrate can be made from a transparent material and the flat interface allows for the use of sensitive optical detection. Sixth, in the cell section part of the microfluidic device, it is possible to integrate a small Peltier heating element over a limited surface to control temperature for optimized culturing of cells on the device.

Microfluidics can be utilized to investigate why individual identical cells, meaning cells originating from the same cell line, same passage number and the same flask respond differently to stimuli. This phenomena is due to the variations of protein expression throughout the cell cycle.[33, 36-41] The causes for these differences are temporal and spatial stochasticity in the chemical processes in the individual cell. Cells studied by bulk methods only give average values for protein concentrations.[35] Individual cells need

to be studied because such studies can yield quantitative data about the natural variation in chemical processes in a cell population and help to identify anomalous cells that have the potential to generate disease. Obtaining data from individual cells will help create a better understanding of the signaling pathways that control important cellular functions in healthy cells

## 2.2 Current Methods for Cell Culturing and Single Cell Analysis on Microfluidic Devices

Microfluidic devices have the potential of becoming the next generation of cell culturing devices, due to the ability of these devices to culture cells in an *in vivo*-mimicked environment. Samples may not behave the same *in vitro* as *in vivo*, however it can be tested using a microfluidic device.[47] Such capability will provide researchers with a platform more comparable in size to the environment of cells in the blood capillaries, than cells cultured in flasks or dishes. One of the major differences of culturing cells in flasks versus microfluidic devices is the mass transfer. Mass transfer under the cell culturing conditions can be due to diffusion or convection. In diffusion, the analytes move from an area of high concentration to an area of low concentration, while in convection the analyte movement is due to change in heat between two areas. Diffusion dominates in the microfluidic channel devices, while convection dominates in a cell culture flask. Convection allows for more rapid exchange of food and waste products and signaling molecules around the cell.

Yu et al. have studied the diffusion in close ranges to the single cells in a microfluidic device versus the tissue culturing flasks.[39] The difference is due to the different condition in the cell culture flask and the microchannel. In a large volume (5-10

mL) of cell culture media there are spontaneous variations in temperature, solute

concentrations and dissolved gas concentration that can lead to surface tension at the

liquid-gas interface. The variations cause rapid convection in the larger cell culture

environments such as a Petri dish or a cell culture flask. In the microchannel, however,

the small dimension of the channels (a volume of 10-100 $\mu$L) minimize convection

because of the very large surface area to volume ratio. Mass transfer, therefore, is mainly

due to diffusion.

The slow nature of diffusion creates a heterogeneous local environment and

chemical gradients around each cell in the microfluidic device due to both food and waste

products surrounding the cell. In contrast, the media around cells cultured in flasks is

moved in both convection and diffusion, thus bring fresh media and creating a more

homogenous environment with less toxic waste products around the cell. (Fig 2.2). Also

signaling molecules important for cell-to-cell communication build up and this important

aspect is lost in bulk culture. The homogenous environment needs to be addressed in

order to successfully culture cells, as will be discussed over the next two chapters.
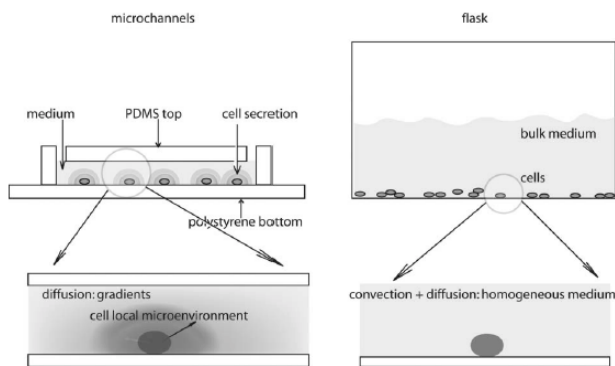


**Figure 2.2 - The different local environments of the cell in microfluidics and flasks.**[39]

### 2.2.1 Culturing of Adherent Cells

Gu et al. (2004) have designed a computerized microfluidic cell culture device with elastomeric channels and Braille displays.[48] The system contained 320 vertical moving pins that were used to power integrated pumps and valves for movement of fluid within an elastic silicon rubber. The computerized fluid controls had three significant advantages. i) the system allowed for rapid mixing between fluid streams. ii) between the mixings, the fluid flow remained laminar and iii) segmented plug-flow of immiscible fluids could be made into a solution flow. The system was used to seed, compartmentalize and sustain C2C12 mouse myoblasts for up to three weeks, however no cell viability was reported. The seeding cells were broken into different compartments by valves where each compartment has its own flow loop. Each loop has an independent pump that transports media to and from the area where the cells are seeded. A typical infusion at 39 h after cell seeding at 15 nL/min is shown in Fig 2.3. The two arrows in the Fig 2.3A show that cells do proliferate better upstream or against the movement of the fluid flow than downstream. The flow rate at which the cells migrate was tested in the range between 3-370 nL/min. At the highest flow of 370 nL/min most of the cells were dislodged. In the flow range of 3-74 nL/min the cell migration was increased when the flow rate was increased. The optimal flow rate used was 74 nL/min where a high cell density can be seen 70 h after seeding (Fig 2.3). This can be compared to the fluid flow of 3 nL/min where the cell density change was not significant except for in the upstream region. Without any flow, the cells died after an overnight incubation, because of the lack of nutrients or growth factors and the build-up of waste products. The Braille display has shown potential as a fluid controller that can be integrated with microfluidic devices

without the need for large and expensive laboratory equipment. Although these are appealing results, the limitation of this cell culture system is that only anchorage dependent cells can be cultured under these conditions.
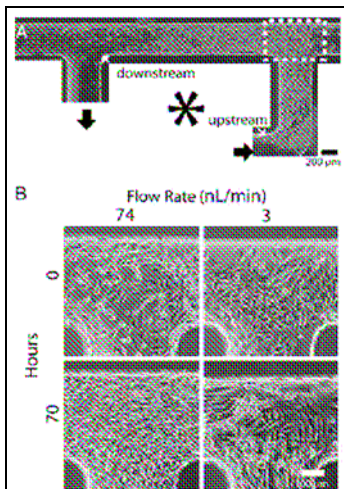


**Figure 2.3 - Gu et al. cell culture design using elastomeric channels and Braille displays for culturing of adhesion cells.[48]**

## *2.2.2 Culturing of Non-Adherent Cells*

Yu et al. (2005) have studied the diffusion in close range to the single cells on a microfluidic device and in tissue culturing flasks.[39] In microfluidic devices the major force generating mass transfer is diffusion, while convection is minimal. This study showed that cells cultured in microfluidic channels had a slower proliferation rate than cells in the cell culture flasks after 24 h. After 48 h the proliferation rate was only 5% in comparison to the cells in the cell culture flask. This is due to the different condition in the cell culture flask and the microchannel. In a large amount (5-10 mL) of cell culture media there are spontaneous variations in temperature, solute concentrations and dissolved gas concentration that can lead to surface tension at the liquid-gas interface.

29

The variations cause rapid convection in the larger cell culture environments such as a Petri dish or a cell culture flask. In the microchannel, however due to the small dimension of the channels (a volume of 10-100 μL), the convection is minimal and the mass transfer is mainly because of diffusion.

Yu et al. (2005) cells in the microfluidic environments where diffusion is the only source of mass transfer start to be affected by the waste products after only a couple of hours.[39] Examples of these products are lactate and acetate, which are acidic products that locally decrease the pH around the single cell. The cells in the microenvironment had a decreased cell growth rate and reached a growth plateau phase earlier than the cells in the flask. This plateau refers to an equilibrium between new cell production and cell death. This was clearly a challenge since there was no overall production of new cells. In Yu's experiment the dimensions of the microfluidic channels were 20 x 1 x 0.25 mm, which was significantly larger than the microwells used in the these experiment. The cells cultured in this channel were Sf9 cells a Fall armyworm ovarian cells (Spodoptera frugiperda insect cell). These cells were chosen because it was a non-adherent cells and free from cell-cell contact inhibition. The cell viability was determined by the use of Trypan Blue, a cell exclusion dye which was taken up by dead cells coloring them with a dark blue color. In this study the proliferation rates were slower after 24 h in the microchannel in comparison to the cells in the cell culture flask. The proliferation rate kept decreasing over the following 48 h reaching a rate of 5% in the microchannel in comparison to the cells in the cell culture flask. The decreasing cell viability in the microchannel was due to the buildup of toxins, since the toxins could only be removed via diffusion instead of convection.

This experiment gives insight into the effects of diffusion of soluble factors in close range to the cells. The limitation of this study is that the local environment of the cell was not receiving fresh media which could help dilute byproducts surrounding the cell which decreased viability.
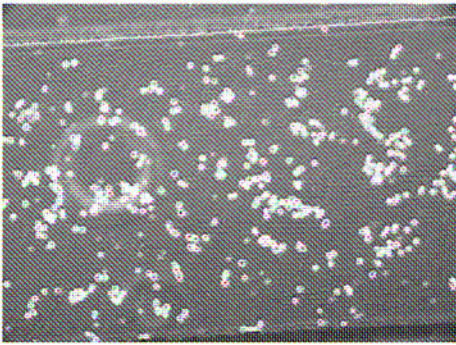


**Figure 2.4 - Yu et al. cultured Sf9 cells a Fall armyworm ovarian cells, Spodoptera frugiperda in a 1 mm long channel.[39]**

Deutsch et al. (2006) have constructed a clever honeycomb design for culturing many individual non-adherent non-tethered single cells.[49] The purpose of this study was to place Jurkat cells in a cell retainer (CR) which has a high density of arrays 2D array of hexagonal picoliter wells in a honey comb-like pattern. This array design is shown in Fig. 2.5. The wells were fabricated in glass with a depth of 8 μm and pitched 20 μm diameter well. The inside of the picoliter well was smooth and the bottom was flat, however the edges of the walls are extremely sharp and less than 0.1 μm wide to prevent cells from settling between the wells. The array wells are arranged in a 100x100 on a glass slide. The cell suspension was loaded using capillary forces at rate of 20 μL/s with a volume of 2 μL cell suspension. The only time viability was mentioned in the experiment was that the cell viability was tested by Trypan Blue and was remained after

loading. The cell viability was not reported and so the usefulness of the device over a long period of time is not known.
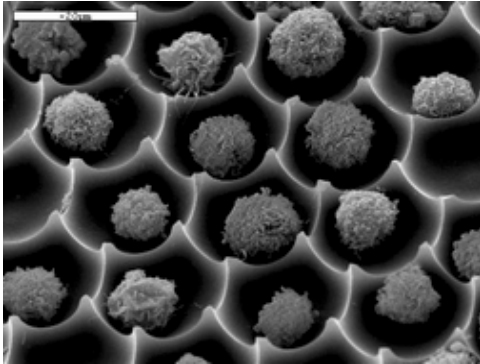


**Figure 2.5 - Deutsch et al. cell retainer (CR) for culturing of single Jurkat cells.[49]**

Di Carlo et al. (2006) have constructed a high density array of hydrodynamic shaped traps for single cell trapping in a robust and simple design.[33, 50, 51] This device has been used for two studies, a study on single cell concentration distributions of carboxylesterases on different cell types and for inhibition of intracellular esterases by the nonspecific inhibitor nordihydroguaiaretic acid (NDGA). The device design is compact, consisting of eight parallel channels with a high density of cell traps in each, the scale bar in Fig 2.6A is 500μm. Cells and media flow enter from the left and are distributed into the eight parallel channels, where the cells gets trapped by the obstacles inside the channels. The traps were made from PDMS bonded to a glass substrate. The obstacles used to trap cells shown in Fig 2.6C. The inside cavity of the traps were varied at 10, 15, 30 and 60 μm. As the trap cavity size was reduced, naturally so were the number of cells trapped. The density of traps is an impressive 3300 single cell traps/mm$^2$. This platform allows for high-quality single cell data which is needed for in depth studies

of quantitative systems. The compact design and simple loading could be used for culturing of single cells, even though no measurement of viability was reported. According to the authors, the PDMS traps were filled in a very short time (<30s) and the device was easy to operate.

Di Carlo et al. (2006) also reported on culturing adherent HeLa cells on the same device with a cell viability over 24 h where greater than 85%.[51] However culturing adhesion cells under constant flow of fresh media is easier, since the cells remain adherent through the experiment. Again, the cell viability was not reported and so the usefulness of the device over a long period of time is not known. The Di Carlo et al. design is closely related to the designs used in the experiments presented in Chapter 4.
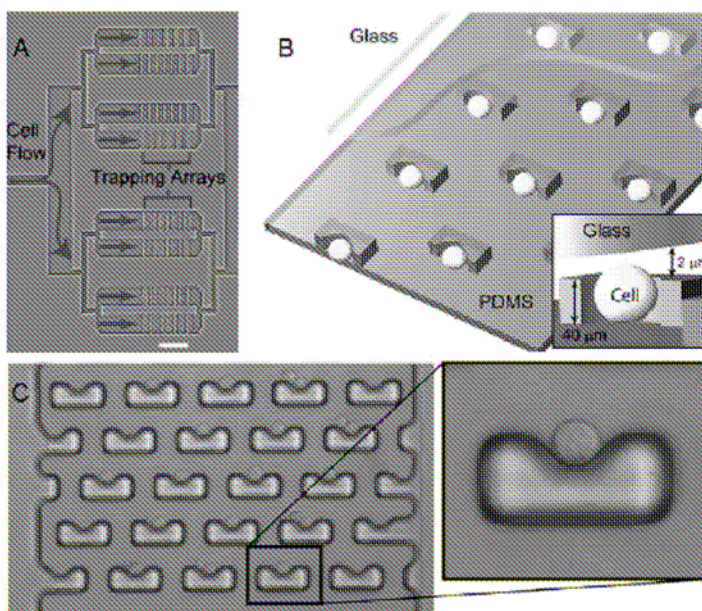


**Figure 2.6 - Di Carlo et al. used a hydrodynamically shaped cellular traps.[51] A. An image showing the device design with 8 trapping arrays. B. Illustration demonstrating how the single cell is trapped between the PDMS and glass. C. Photomicrograph of the individual traps holding individual cells.**

## 2.2.3 Single Cell Analysis using Capillary Electrophoresis and Microfluidic Devices

Li et al. (1997) have studied the mobilization of biological cells on a microfluidic device.[52] This device was tested with *Escherichia coli*, *Canine Erythrocytes* and *Saccharomyces cerevisiae*. The cells were transported using electrokinetic and electrophoretic flow. All the cells had a negative charge which caused a migration to the anode in an electric field. However in an uncoated glass device the electrophoretic mobility was smaller than mobility due to electroosmotic flow, which caused the cells to migrate toward the cathode. The cells can be transported in an even direction by the changing the voltages from loading mode to injection mode. At loading the cells migrate at a velocity of $0.18 \pm 0.02$ mm/s. Under these steady state conditions an injection plug can be formed at the intersection. By switching the voltages in the channels the plug was injected at a velocity of $0.16 \pm 0.02$ mm/s into the main channel (labeled W for waste in Fig. 2.7). The highest velocity was $0.49 \pm 0.08$ mm/s, when the field strength was 160 V/cm. This system used field strength typically at 100 V/cm, but ranged up to 600 V/cm. These field strength should not damage the cell membrane, however high electric field strength was used to form electroporation to introduce labeled substances or DNA to the cells. This process occurs at 1 kV/cm for *Escherichia coli*[53], 2-4 kV/cm for human erythrocytes[54] and 5-10 kV/cm for *Saccharomyces cerevisiae*[55]. In this report cell damage should not occur and this was not studied in detail. However they did notice cells directly in the double-layer region of the electrode used to apply the potential to be lysed.  Also as

the field strength increased, so did the cell velocity, which made it difficult to image cellular damage due to low resolution of the camera.

To illustrate that this device can be used for cell lysis, a stream of erythrocytes were mixed with a stream of a chemical. For a sufficiently rapid lysis the anionic detergent sodium dodecyl sulfate (SDS) was used. Fig 2.7A shows the erythrocytes are mixing with a 3 mM SDS solution. According to the authors Fig 2.7B shows cell 1 and 4 are starting to react to the SDS. The SDS does not diffuse evenly over the channel, which leaves cells 2 and 3 intact. Fig 2.7C shows that cell 1 has migrated out of the image, but that cells 2, 3 and 4 have been lysed.
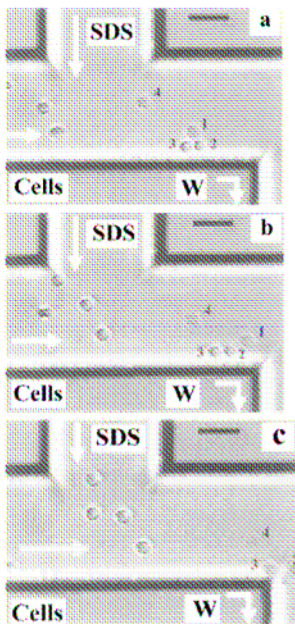


**Figure 2.7 - Photomicrographs of erythrocyte (numbers 1-4) cell lysis in a microfluidic device. The white arrows in the images indicate the fluid flow direction. The black scale bar in the upper right corner is 20 $\mu$m.**

Sims et al. (1998) have reported on a laser-micropipette system (LMS) for analysis of single adherent cells (Fig 2.8).[46] In this technique single rat basophilic leukemia (RBL) cells were loaded with a fluorescein diacetate and/or Oregon Green diacetate. The cells were washed with a physiological extracellular buffer, then labeled in a solution of fluorescein (20 nM) and Oregon Green diacetate (500 nM) in physiological extracellular buffer with glucose (10 mM). The cells were incubated in room temperature for 30 min, to allowing for fluorescent labeling. The cells were washed continuously by a 10 mL/min to reduce excess background fluorescence.

This was followed by a fast cell lysis of adherent single cell by using a frequency doubled Q-switched Nd:YAG laser to generate a single laser pulse into a fluorescent microscope. The laser beam was focused through the microscope objective to a position of 20-30 μm within the cover slip with the single cell.[56] The shock wave from the laser caused the cell membrane to be completely disrupted. A CCD camera was used to monitor the cell lysis every 33 ms. After cell lysis the capillary had to be rapidly and manually moved 15-25 μm above the cell in order to inject the lysate. After the injection the capillary was moved manually from the cell, placed in running buffer to start electrophoresis and the cell lysate was detected by laser induced fluorescence. Following each cell lysis experiment the capillary needed to be rinsed for 10 min, which makes this technique time consuming.

Although this is a very impressing technique, it does require very specific measurements. The adhesion cell (10-50 μm ) needed to be placed 20-30 μm from the laser beam and the capillary was placed 15-25 μm above the cell after lysis to perform

single cell analysis. This system does require specifically trained personal and tend to be very time consuming for analysis for a high population of single cells.
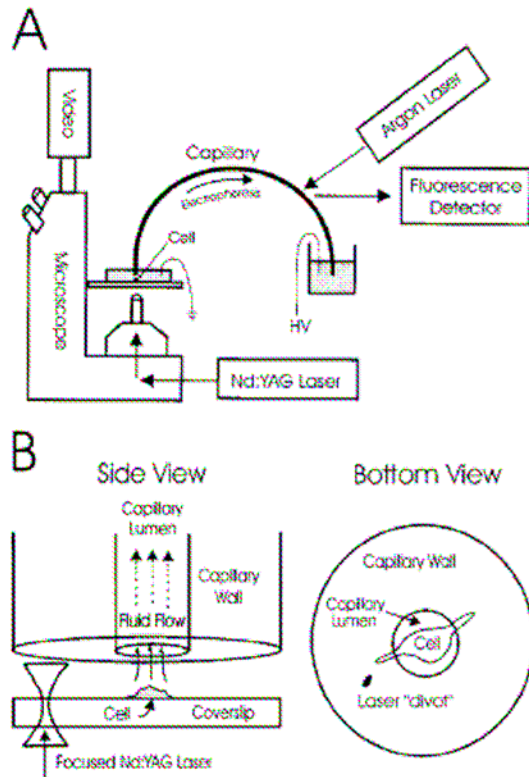


**Figure 2.8 - A .Sims et al. experimental setup for single cell analysis using a laser-micropipette system[46] B. A close-up on the side view and bottom view of the single cell prior to lysis.**

Wheeler et al. (2003) have reported on a poly(dimethylsiloxane) device integrated with 8 actuating valves and 6 pumps to isolate a single cell for assays studies.[57] The device can be used for rapid isolation of single cells from a mixture and to delivery precise volumes of reagent to a single cell. This microfluidic device allows for precise and gentle guidance of single cells as they are transported from bulk solution to the dock. Eight actuating valves used by applying pressure to the control inlets (Fig. 2.9A shown as V1-V8) are used to move the fluid by the six pumps (P1-P6). The five reactant inlets (R1-

37

R5) allows for single cell assays directly on the device. There are also ports for shielding

buffer (SB) and focusing buffer (FB). The cell is guided between two hydrodynamic

focused streams to the dock where the assay takes place. The dock have small draining

channels (see the arrows in Fig 2.9B) prevents the dock from overflowing. Even at high

velocities as 1 mm/sec the cell lands gently inside the dock. Reagents are "loaded" a few

micrometers from the single cell. The reagents are allowed to perfuse into the single cell,

to terminate loading a shielding buffer is added to the fluid around the cell. A Fluo-3

assay was performed on Jurkat cells in the cell docks. Fluo-3 is a calcium-indicating dye

which measures the calcium concentration. The reagent was added in close proximity to

the cell. The dye was taken up by the cell with excess dye rinsed away. This loading was

advantageous, usually labeling procedures require additional washing steps which were

not needed here. This reduces experimental time and reduces the stress on the cell. The

dock trapping is interesting and several assays can be performed on single cells, however

the limitation is the low throughput, which makes the technique very time consuming.
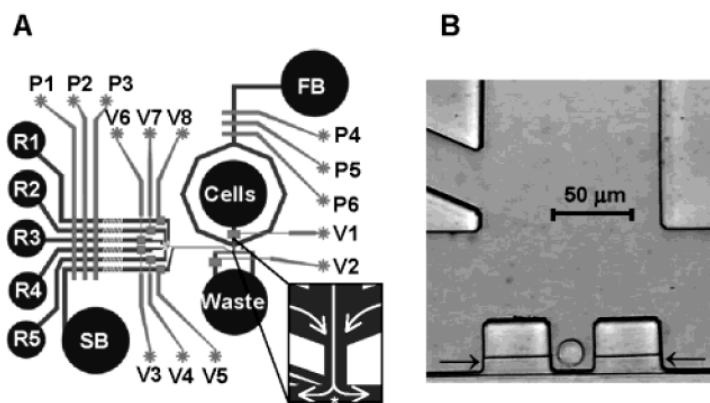


**Figure 2.9 - Wheeler et al. have designed a device for single cell assays using PDMS.
A. An illustration of the fluidic device with eight valves and six pumps for fluid
control. B. A CCD image of a Jurkat cell trapped in the dock prior to analysis.**[57]

McClain et al. (2003) have reported on the most impressing single cell analysis to date.[58] A microfluidic device with integrated: cell handling, rapid cell lysis and electrophoretic separation (Fig.2.10). This device has a high-throughput of 7-12 cells/min which are >100 times faster than methods using standard bench-scale capillary electrophoresis. In this experiment Jurkat cells were loaded with oregon green carboxylic diacetate or calcein AM. The fluorescently labeled cells were transported by hydrodynamic flow from the cell sample reservoir, focused and rapidly lysed using an electric field. The lysate were automatically injected into the separation channel and detected 3 mm from the intersection. The separation time was 2.2 s and the efficiencies ranged from 2300 to 4000 theoretical plates.

A limitation of this experiment was the use of a highly conductive extracellular buffer, which leads to gas formation due to Joule heating. The extracellular buffer was needed to provide the cells with an isotonic medium, to reduce cellular stress. Alterations to this buffer could prevent band broadening due to Joule heating and the separation efficiency could be improved.
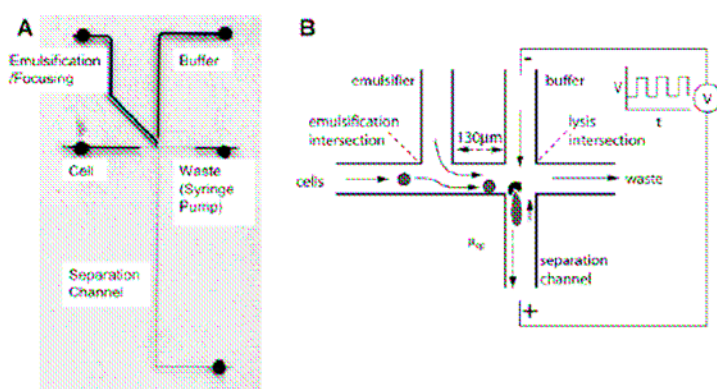


**Figure 2.10 - McClain et al. microfluidic device for single lysis and analysis.[58]**

Gao et al. (2004) have a microfluidic device with integration of cell sampling, loading, docking, lysis and capillary electrophoresis.[59] Single human erythrocytes were tested on this device. Glutathione (GSH) was used as a model for intracellular compounds. The cells were transported under hydrostatic pressure because of different liquid levels in the reservoirs. Cells floated from the sample reservoir (S) to the sample waste (SW) as indicated by the white arrows in Fig 2.11A. As the cell approached the intersection electrical potentials were applied over the reservoirs. The sample cell was guided by the electroosmotic flow (EOF) toward the buffer reservoir. Since the EOF was greater than the hydrostatic flow the cell will be transported in the direction of the EOF. In the initial results of these experiments the electric field strength was ranged from 100 V/cm to 800 V/cm. However at 100 V/cm the cells were not transported and when the field strength exceeded 600 V/cm the cells were lysed in the sample channel.

After 2 s the potentials were switched on and off for 2-3 times with an interval of 1 s. This fast iteration of flow direction caused the cell to dock with the channel (Fig 2.11B). At 15 s after the docking electrical fields of 280 V/cm were applied for 40 ms and the cell was lysed immediately (Fig 2.11C). After lysis the labeled intracellular components were released, separated by capillary electrophoresis and detected by laser induced fluorescence detection. The average cellular concentration of GSH in human erythrocytes was found to be $7.2 \times 10^{-4} \pm 3.3 \times 10^{-4}$ M. The throughput of this device was 15 cells/h.
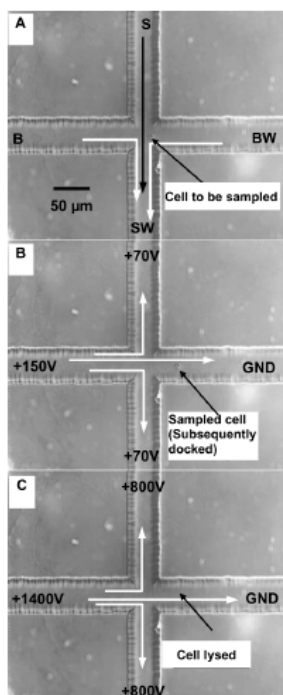
**Figure 2.11 - CCD images of single erythrocyte was loaded (A), injected into the separation channel (B) and lysed using an electric field in 40 ms.**[59]

When I started this project in 2004 the field was mainly focused upon the transportation of single cells through microfluidic devices and the separation and characterization of fluorescent molecules release from these cells after lysis. Information about culturing single cells on microfluidic devices was limited. We wanted to build a microfluidic device for culturing of single cell, how we did this will be discussed over the next two chapters.

# CHAPTER 3 – CELL CULTURING ON A MICROFLUIDIC DEVICE WITH PERIODIC MEDIA REPLACEMENT

## 3.1 Introduction

As stated in the introduction the aim the overall goal of this project was to develop methods to culture single non-anchorage dependent cells inside a microfluidic device, release the daughter cells into a flowing stream above the cultured cell array, load the cells with a fluorescent substrate and perform single cell analyses. The individual cells have discrete molecular, metabolic and proteomic identities which interconnect with other cells[32] which can be investigated by single cell analysis. This chapter will focus on exploring 2 novel techniques to perform cell culture within a microfluidic device.

As the cells that we are interested in are non-adherent, methods must be developed to first capture the cells and then to successfully culture them. Not only do the cells need to be cultured, but some of the daughter cells need to be able to be released from the array. One potential method to successfully accomplish all three of these goals – capturing, culturing and releasing some daughter cells is shown in Fig 3.1 In this method, cells would be drawn into a device that consists of an array of wells about the size of the cells. The cells would then gravitationally settle into the wells and be cultured. As the cells then grow and eventually undergo mitosis one of the daughter cells would be pushed up into a flowing stream above the array of cells and transported to a location where further analysis could be performed.

The goal was to have a cell released on average every 5-10 s. This could be achieved if the device had 20,000 wells filled with cells which have a doubling time of 48

h. The cells would go through random cell division over 2880 min (48 h x 60 min= 2880 min) and produce another 20,000 cells. The number of cells produced per min is 20,000 cells/ 2880 min= 7 cells/min. The time per cell release is calculated by: 60 s/7 cells= 8.5 s/ cells. The ability to release a cell approximately every 8 s is the motivation behind fabricating a device with 20,000 wells. It would be difficult to have all 20,000 wells within one large single channel because the PDMS material could collapse. Therefore, these wells were divided into 8 parallel channels, where each channel contained an array of 2,500 wells, which makes 8 x 2,500 wells = 20,000 wells.

If the cell traps are shallow enough to hold only one cell then one of the daughter cells will be forced out of the well after cell division. This scenario is pictured in Fig. 3.1, where the cell in the trap and goes through cell division. After the division there are two daughter cells inside the traps, but because of the narrow confinement in the well one of the cells will be pushed out and will move with the media flow towards single cell analysis.
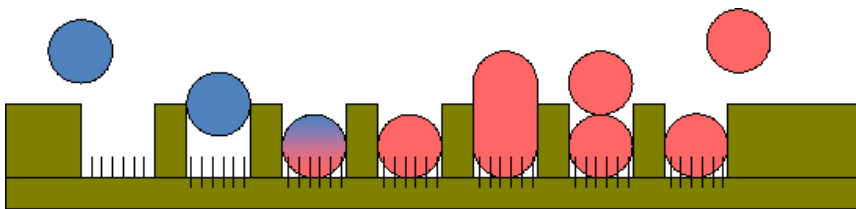


**Figure 0.1 - The objective for experiment was to trap single cells, allow it to go through cell division and then cause one daughter cell to be transported for single cell analyses.**

A sketch for a device capable of capturing, culturing, and releasing cells integrated with microfluidic components that would allow further analysis of the cells released from the array is shown Fig. 3.2. First, the cell is cultured in the green arrays shown to the left in Fig. 3.2. The daughter cells are transported to the loading site (blue mark in Fig 3.2) where a fluorescently tagged protein is added to the cell. After labeling, the cell is transported to the separation area where the cell would be lysed and the contents separated electrophoretically and finally detected using LIF.
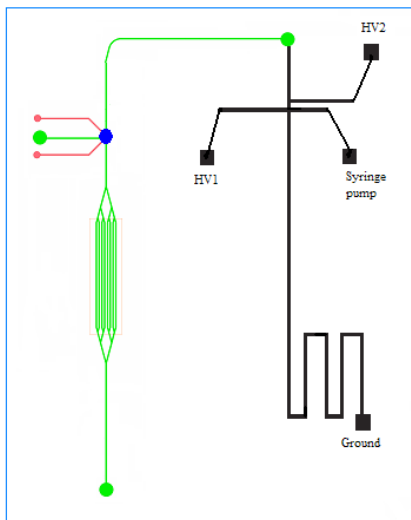


**Figure 0.2 - The schematics of the device for single cell culturing, labeling and lysis.**

### 3.1.1 Using Poly(dimethylsiloxane) (PDMS) for Cell Culturing

PDMS is a polymer widely used for fabrication of microfluidic devices.[60] To culture cells on microfluidic devices it is essential that the material is biocompatible[61-64], meaning that the material does not release toxins and is gas permeable and thermally stable. PDMS is also optically transparent which means that cells can be observed continuously. Analytes in or released from cells can be detected visually or fluorescently.

44

PDMS has a high electric resistance which is needed for high efficiency electrokinetic separations and so would be compatible with downstream analysis, i.e. electrophoretic separation of the contents of the released daughter cells. The fabrication for the devices is rapid, facile and inexpensive. One potential limitation of using PDMS to make microfluidic cell culturing devices was the hydrophobicity of PDMS. However the surface can be treated to reduce that effect, which will be explained in the following section.

## 3.2 Experimental Setup

### 3.2.1 Chemicals

Jurkat Clone E6-1 (lymphoblast) cells were purchased from the American Type Culture Collection (Manassas, VA). Cell media RPMI-1640, Phosphate buffered saline and isopropanol were obtained from Fisher Scientific (Pittsburg, PA). Bovine Serum Albumin (BSA), Human Fibronectin (HFN), Calcein AM and Propidium iodine were purchased from Invitrogen (Carlbad, CA). SU-8 2035 and SU-8 Developer, 453 Microposit Developer were obtained from MicroChem (Newton, MA). poly(dimethylsiloxane) (Sylgard®184 Dow Corning, Midland MI. The Pentane was purchased from Sigma Aldrich (St. Louis, MO). Triethylamine and ethylacetate were obtained from Fisher (Pittsburg, PA). Distilled deionized water was obtained from Barnstead Ultra pure Water System (Dubuque, IA) and filtered with a 0.45 μm Millex®-LCR syringe driven filter (Millipore Cooperation, Bedford, MA). Argon gas was obtained from Linweld (Manhattan, KS). All chemicals were used without further purification.

### 3.2.2 Polymer Microfluidic Device Fabrication

The design and fabrication of the master mold were previously described in section 1.3.2, The polydimethylsiloxane was mixed in the ratio 10:1 of the polymer to curing agent. The mixture was degassed in a vacuum desiccator for 30 min, before it was poured on the master mold. The device was placed in an 80° (Lindberg/ Blue Mechanical Convection Ovens) oven for 30 min. After curing the device was carefully removed from the master mold.

### 3.2.3 Cell Line

Jurkat Clone E6-1 (lymphoblast) was purchased from the American Type Culture Collection (Manassas, VA). The ATCC recommends the Rosemary Park Memorial Institute (RPMI-1640) medium for the Jurkat cell.

For a brief period of time an alternative cell culture media was tested, the Lebovitz 64 media as it allows cells to be cultured in an environment less dependent on elevated $CO_2$ levels.[65] This would be advantageous for culturing the cells in a portable device, however the cell viability was 80% when cultured in the Lebovitz media. In the experiments reported here were all made using RPMI-1640 as the cell culture media, where the cell viability was usually 95-98%. The cell viability testing is explained in detail in section 3.2.3. The cell passages for these experiments were 2-35.

### 3.2.4 Cell Imaging Techniques

Cell images for determining viability were performed using a Roper Scientific CCD camera (Princeton Instruments Inc., Trenton NJ) and an inverted microscope, (Nikon Eclipse TE 2000-U, Melville, NY) was used to image the cells. The inverted

microscope was incorporated with an epiliuminescence system, using a 500 W Mercury arc lamp with blue and green filter cubes for the excitation of dyes with excitation wavelengths similar to fluorescein and rhodamine derivatives.

### *3.2.5 Cell Viability and Filling Rate Calculations*

Before the cell culturing experiments the cell viability was tested with Trypan Blue. This was a non-fluorescent dye; instead it has an intense dark blue color. If the cell membrane has been compromised this blue die passed through and labels specific proteins inside the dead cell. When imaged on the inverted microscope it was found that dead cells have a distinct blue color, while the living cells have are without color. To perform the viability test a small aliquot of cells was loaded into an Eppendorf tube. The cells were mixed 1:1 with Trypan Blue and loaded onto a Haemocytometer[25] The ratio of alive to dead cells was determined and the cell viability and seeding density was calculated.

Calcein AM is fluorogenic, which causes it to diffuse passively through cellular membranes. Once it is inside the cells esterases in the cell cleave the acetoxy groups making the molecule fluorescent and charged. Because of the charge the molecule can no longer passively diffuse through the cell membrane. The fluorescent dye remains inside the cell, but will slowly leak out over time with anionic transporters.[66] A second fluorescent dye is propidium iodine, that we excite wavelength at 515 nm was used to label dead cells. It diffuses through cell membranes that have been compromised and labels the DNA in the cell nuclei in dead cells. For cell viability measurements using fluorescent dyes, a mixture of calcein AM and propidium iodide in a phosphate buffered saline solution was prepared, according to the recommended protocols from Invitrogen.

This solution was rinsed over the cells for 3 min. The cells were then incubated with this solution for 10 min to generate reproducible results. The cells were imaged on an inverted microscope (Nikon Eclipse, Inverted microscope TE2000-U, Melville, NY) over the exact same area (Fig 3.8).

The cell viability was investigated by imaging $500 \pm 25$ fluorescently labeled cell inside microfluidic traps at each endpoint. Propidium iodide labeled cells was counted as dead cells and the non-propidium iodine labeled cells were counted as alive. The cell viability in percent was calculated by dividing the number of alive cells over the total number of cells and multiplied by a factor of 100.

The filling rate was determined by calculating how many traps had no cells or one cell or more inside over 500 traps. The percent filling rate was calculated by dividing the number of cells with one or more cells over the total number of wells counted and multiplied by a factor of 100.

### 3.2.6 Maintaining a Sterile Environment

Since eukaryote cells have a longer doubling time than prokaryote cells (bacteria), it was very important to keep the microfluidic environment sterile when performing the cell culturing. To prevent bacterial contamination the following steps were taken: All manipulations of media, cell, solutions and the experimental setup were made in a biological hood or on a clean bench. The media contained the antibiotics, penicillin and streptomycin. The device was exposed to UV-light for 30 min to sterilize the surface before cells were added. Only sterile syringes, pipettes, flask and Eppendorf™ tubes were used for all cell culturing experiments.

# 3.3 Results and Discussion

## *3.3.1 Treatment of PDMS for Cell Culturing Devices*

Initial attempts of filling the device were especially difficult due to bubble formation, so the PDMS was extracted to improve the wettablility. PDMS has highly advantageous properties (discussed in section 3.1.1), however two limitations to culturing cells on PDMS are the hydrophobic surface which complicates the loading of aqueous media[67] and the low molecular weight oligomers within the material that can negatively effect the health of the cells[68]. These two issues were addressed by treatment to the polymer. The hydrophobic surface of PDMS is due to the repeating unit of -O-Si$(CH_3)_2$- groups. This chemical structure creates a hydrophobic surface. The literature values of the water contact angle for PDMS ranges between 110°-100°. The surface can be made hydrophilic through air plasma treatment which destroys the methyl groups in the surface Si$(CH_3)_2$ and forms the Si(OH) which gives the surface a hydrophilic character. A disadvantage is that if the device is in contact with air, the surface rearrangement will bring new hydrophobic groups[69] to lower the free energy of the surface. To reduce the probability of regenerating hydrophobic channel walls, the devices are extracted in organic solvents. This causes the polymer to swell and low molecular weight oligomers are washed out of the PDMS. After the extraction and 90 s of air plasma treatment the surface does remain hydrophilic. The measurement of the relative hydrophobicity and hydrophilicity of the walls was measured by the water contact angle. If a surface is hydrophilic, a droplet of water will spread evenly over the surface yielding contact angles that are <90°. A water contact angle measurement less than 90° defines the material as hydrophilic.[70]

Two approaches were attempted to reduce the amount of these unreacted oligomers. The first method attempted to extract the low molecular weight oligomers from the completed PDMS devices required the PDMS to be soaked in pentane for 24 h, transferred to acetone for 24 h, dried with Nitrogen gas and finally dried in a 90°C oven for 24 h.[68] Unfortunately, this method was very time consuming. A second faster and easier method was found in which the PDMS was soaked in triethylamine for 2 h, and then switched to a solution of ethylactetate for 2 h and finally acetone for 2 h.[67] After extractions the devices were dried in a 65°C oven for 2 h and finally exposed to air plasma (Plasma Cleaner PDG-32G Harrick Plasma, Ithaca, NY) for 90 s. The water contact angle was reduced from 105°± 2° on the native PDMS to 41°± 2° after extraction and air plasma treatment shown in Fig 3.3. This increased wettability of the PDMS surface helped considerably when solutions and cells were loaded to the device.
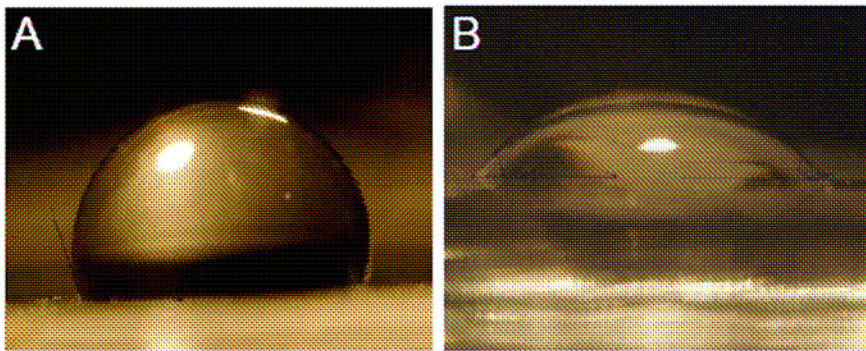


**Figure 0.3 - The water contact angle (A) before and (B) after the air plasma treatment of extracted PDMS.**

**Table 1 - The water contact angle measurement for natural and treated PDMS.**

| PDMS | Natural | Plasma treated |
|---|---|---|
| Water contact angle | 105°± 2° | 41°± 2° |
| Number of replicate data (n) | 5 | 5 |

### *3.3.2 The Microfluidic Device for Cell Culturing*

In order to culture cells successfully on microfluidic devices a variety of specific characteristics need to be designed into the device. First, this device we need to have 20,000 cell traps in order to achieve the cell analysis rate of producing one cell approximately every 10 s, as discussed in section 3.1. Second, the 20,000 wells have been divided over eight parallel arrays, where each array contains 2,500 wells. The reason we have eight parallel channels rather than one large channel is that wide channels fabricated in PDMS will collapse due to the flexible nature of PDMS. Third, two loading reservoirs are needed in order to introduce and remove cells and solutions onto the device.

The PDMS (channel layer and cell trap layer) and Plexiglas® plates were sterilized by placing them inside a Petri dish and exposing them to UV-light in the biological hood for 30 min. To ensure a sterile environment for the PDMS device a stereoscope and the motorized hamster wheel were cleaned with Kimwipe® soaked in 70% ethanol and placed the in laminar flow bench to be clean from dust particles.

After sterilization the channel layer and cell trap layer were alignment under the stereoscope to ensure a secure assembly. The left side of the figure Fig 3.4 shows the entire microfluidic device. The length of the eight parallel arrays were 1 cm and are branched together on each side to two loading channels which leads to cubic shaped reservoirs. The total volume the entire device was 5-10 µL. A close-up to the right in Fig 3.6 shows the channel branching into the eight parallel arrays that contain the cubic shaped cell traps.
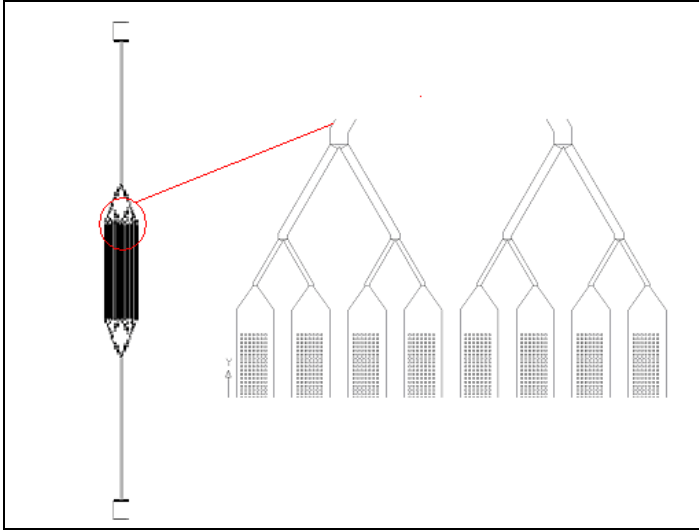
**Figure 0.4 - The left side of the figure shows the AutoCAD sketch of the entire microfluidic device with eight parallel arrays branching into two cubic shaped loading ports. The right side shows the loading port branch into eight parallel arrays with the cubic shaped cell traps.**

The PDMS device was sealed between the Plexiglas® covers, with the dimensions of 10 x 15 cm and held together by four screws (Fig 3.5). The covers had two main purposes; First, the stiffness of the Plexiglas® created an even pressure over the PDMS cell culture area of the device; this prevented leakage problems. Second, the top Plexiglas® holder had two drilled holes in it. These holes were lined up with the loading ports on the PDMS devices, so the compartments in the Plexiglas® could be used as reservoirs. These reservoirs had to hold approximately 100 µL solution, which made it convenient for loading and removal of solution. The loading solutions were added to one of the two reservoirs while the second reservoir was connected to a vacuum system, so that solutions could be pulled very slowly through the device.
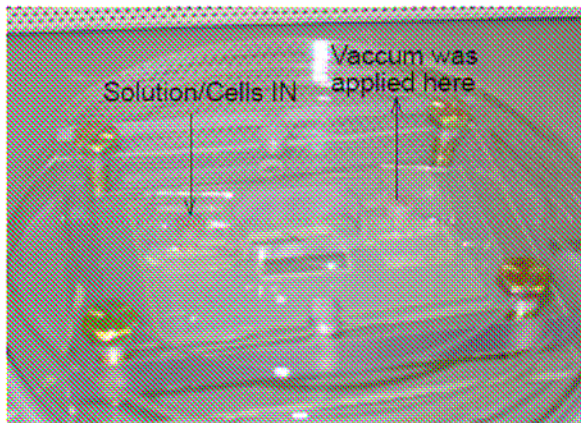
**Figure 0.5 - The cell culture device for periodic media displacement.**

The extraction and air plasma treatment (section 3.3.1) did create a less hydrophobic PDMS surface, but it was still challenging to fill the channels. To improve the wettability the channels were filled with a polar organic solution, in this case ethanol. First the channel network was filled with 96% ethanol to ensure that the channels filled completely for 3 min. Then a 50% ethanol solution was rinsed through the channels for 3 min. Finally the channels are rinsed with double distilled water for 3 min. Bovine serum albumin (BSA) and human fibronectin (HFN) were used to coat the PDMS for 10 min each to create the surface more suitable for the cells. Whenever the BSA and HFN were used in the experiments reported below, they will be specifically reported.

After the cell viability had been confirmed to be > 95% in the cell culture flask, a 2 mL cell sample was retrieved from the same flask in the cell incubator. The sample was centrifuged for 1 min at 800 rpm and resuspended in fresh media to a seeding density of $1 \times 10^6$ cells/mL. The cell sample was loaded into the channel network through the loading ports shown in Fig 3.5 and the cells where transported by a low vacuum flow

to fill the eight parallel arrays. After filling the device was placed on the motorized

hamster wheel to centrifuge the cells at 60 rpm for 5 min.
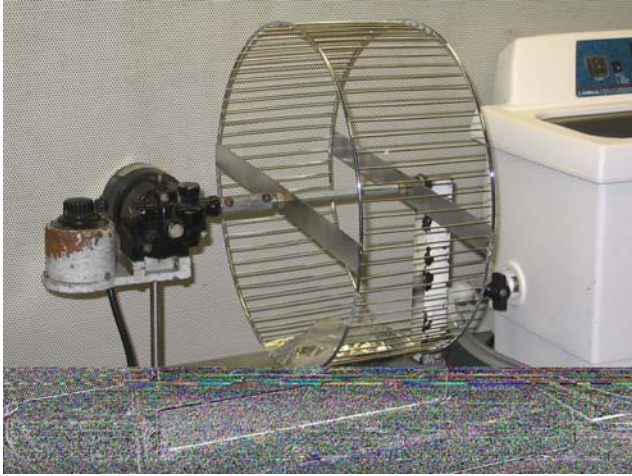


**Figure 0.6 - The motorized hamster wheel used to load the cells into the traps.**

The centrifugal force generated motorized hamster wheel did not damage the cell

according to the cell viability testing performed right after loading. The result of the cell

viability test with calcein AM and propidium iodide is shown in Fig. 3.7.

The viability was > 95% (n = 4) when tested by calcein AM (Fig. 3.7A.) and

propidium iodine (Fig 3.7B). This was perfectly normal as there are always some dead

cells from the cell sample taken from the cell culture flask. It was found that calcein AM

can give a false positive result for live cells, due to wide excitation spectra, the calcein

AM was excited by the excitation wavelength used for propidium iodine. All the cell

viability measurements, therefore, were based on propidium iodide labeling.
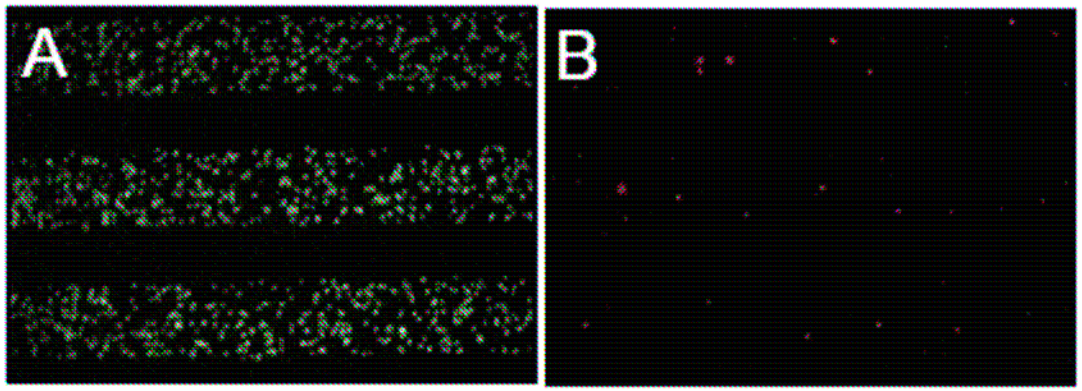
**Figure 0.7 - This image shows three arrays with Jurkat cells right after the centrifugation. The two images are over the exact same area showing A) Calcein AM labeled cells and B) Cells labeled with by propidium iodine.**

The entire microfluidic channel design with the eight parallel arrays can be seen in Fig. 3.8A, under a 4X microscope magnification. A close up of the calcein AM labeled cells inside the channels branching can be seen in Fig 3.8B under a 10X magnification. The calcein AM labeled cells caught in the cubic shaped traps is shown in Fig. 3.8C under a 60X magnification.
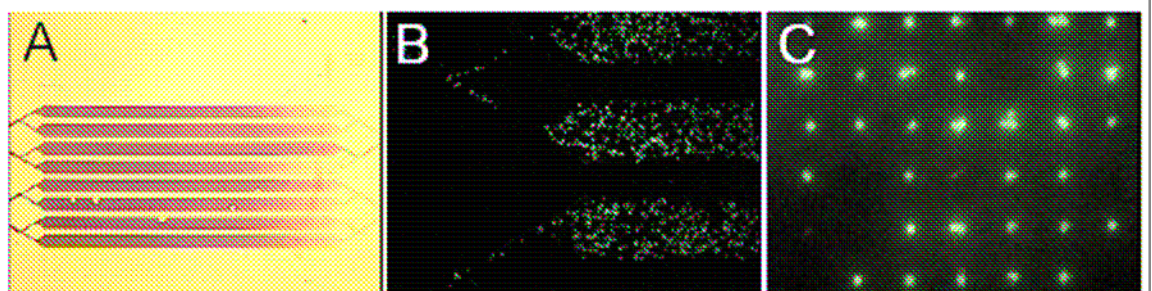


**Figure 0.8 - A. The entire microfluidic device filled with Trypan Blue shows with 8 parallel arrays under a 4X microscope magnification. B. A close up of the calcein AM labeled cells being loaded into the arrays under a 10X magnification. C. Calcein AM labeled cells remain in the cubic shaped traps under a 60X magnification.**

The Plexiglas®/PDMS device was placed inside a large Petri dish with 10 mL of double distilled water[71] to maintain the humidity in the local environment of the device. The Petri dish was then placed inside the incubator set at 37°C with 5% $CO_2$ in air. In the initial experiment without the humidified cell viability after 12 hrs was 0 (n = 3).

### 3.3.3 Cubic Shaped Cell Trap Arrays

Initially cells were cultured inside cube-shaped cavities made from PDMS.[72] These traps were 20 μm deep, 20 μm wide and 20 μm long, as shown in Fig 3.9. The volume of the cubic trap was 8000 $\mu m^3$. This volume is about 8 times that of the average cell volume. Although the initial wells were larger than what will eventually be needed we wanted to optimize the cell culturing conditions first and then decrease the well size. The filling rate after loading of these traps was 63 ± 16% (n = 3).
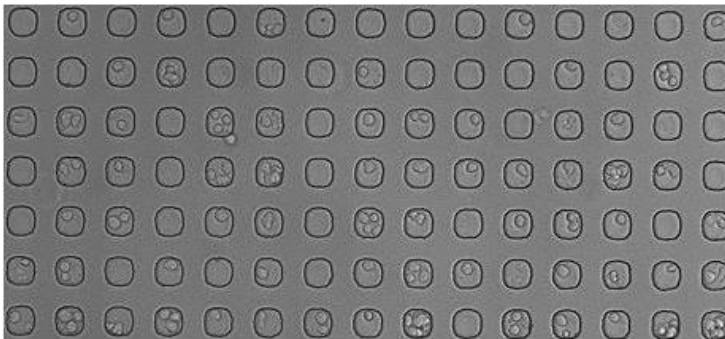


**Figure 0.9 - A CCD camera image of Jurkat cells inside the cubic shaped traps.**

### 3.3.4 Cell Culture Experiments for 48 h under Periodic Media Displacement

Our initial cell culture experiment was performed on a non-extracted PDMS for 48 h. This resulted in a cell viability of $1 \pm 2\%$ after 48 h (n = 5). In order to try to improve the cell viability, a variety of variables were modified as explained below. At first the cells were cultured in the PDMS without Plexiglas® covers. Without the covers, the device leaked media during culturing. In addition to preventing leakage the top Plexiglas® plate opening was utilized as a reservoir for solutions, which made loading of solutions easier. Another issue was filling the PDMS without bubble formation, to improve the filling we started extraction experiments followed by air plasma treatment to increase the wettability of the surface. We also found that the extractions removed low molecular weight oligomers, which further increased the cell viability.[61] PDMS is often characterized as a biocompatible material,[61-64] but to culture cells long-term the polymer need to be extracted from low molecular weight oligomer as discussed in section 3.3.2 and coated with bovine serum albumin (BSA). An additional concern was media evaporation during culturing, this was prevented by placing the Plexiglas®/PDMS device in a large Petri dish with 10 mL of double distilled water[71] to maintain the humidity in the local environment of the device. This prevented the media from evaporating and as a result of this the cell viability increased.

The improvements resulted in a cell viability of $72 \pm 5$ % (n = 3) after 48 h of culturing. The cell viability was increased further by using PDMS that was extracted and coated with BSA and human fibronectin (HFN). The HFN was added in an attempt to create a more biocompatible surface. The result after 48 h was $79 \pm 6$ % (n = 3) as shown in Fig. 3.10. This is a higher viability than has been reported previously.[39]
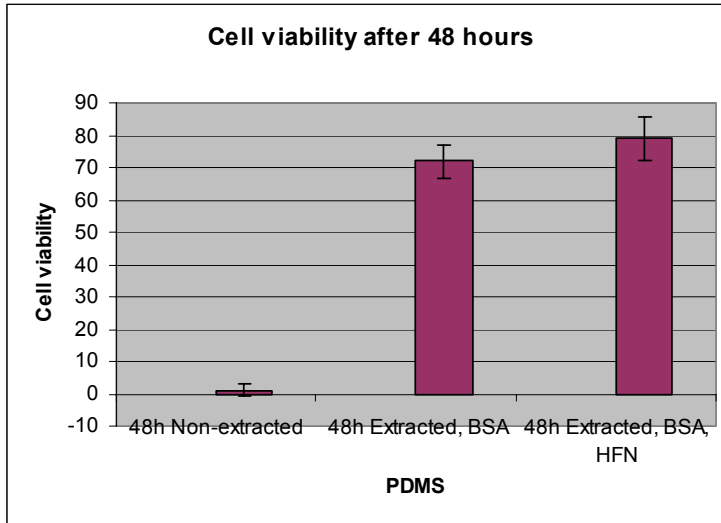
**Figure 0.10 - Result for 48 h cell culture experiment under various preparations to the PDMS. The initial result on un-treated PDMS was $1 \pm 2\%(n = 3)$. After extracting the PDMS and coating the surface with BSA the result was $72 \pm 5\ \%(n = 3)$. With the addition of HFN on the surface the viability was $79 \pm 6\ \%.(n = 3)$**

The challenge with this 48 h experiment was that the media had to be refreshed every 6 h, in a process that could potentially introduce contamination. To load the new media the old media was removed from the reservoirs on the device using a sterile syringe. Fresh pre-warmed media was added using a second sterile syringe. The cell viability was tested using calcein AM and propidium iodine, to load the dyes the device was transferred from the incubator and to the laminar flow hood. The dye-mixture was added to the device and rinsed over the surface with a low vacuum flow. The device was then transferred to the inverted microscope to estimate the viability of 500 cells. Due to the high risk of contamination and the laborious nature of the procedure, we wanted to develop a better design which will be discussed in Chapter 4.

## 3.4 Conclusion

In this chapter Jurkat cells were cultured under static conditions on a PDMS microfluidic device. The polymer was extracted to reduce the amount of low molecular weight oligomers and treated with air plasma to generate a biocompatible hydrophilic surface. The initial cell culturing results were poor with a cell viability of only $1 \pm 2$ % (n = 3) after 48 h culturing. After performing the extractions of the PDMS and coating the channel with BSA, however, the viability increased dramatically to $72 \pm 5$ % after 48 h. A further increase in cell viability to $79 \pm 6$% (n = 3) was observed as the extracted PDMS was coated with BSA and HFN. The filling rate after loading of these traps was $63 \pm 16$% (n = 3). These cell viability results were higher than any previously reported.[39]

However, this experiment was very difficult to perform as the addition of media to the cells risked the sterile integrity of the system and the cubic traps holding the cells were too large to generate the release of daughter cells as we wanted. Attempts to solve some of these limitations are explored further in Chapter 4.

# CHAPTER 4 - CELL CULTURING ON A MICROFLUIDIC SYSTEM UNDER CONTINUOUS MEDIA PERFUSION CONDITIONS

## 4.1 Introduction

After demonstrating that we could successfully culture non-adherent cells on microchips for 48 h in Chapter 3, we wanted to improve the cell culturing system further so that it could be integrated into a single cell analysis system. Therefore, in this chapter we report the development of two new cell trap designs with smaller wells that have the ability to trap individual cells.

One of the cell traps types have a circular shape with a inner diameter of 13 µm have 2 µm narrow channels connecting to the traps. These narrow channels allow the cells to send and receive signaling substances the neighboring cells. We hypothesize that this might be important, since it has been reported that cell-to-cell (i.e. paracrine) signaling, helps to promote cell health and growth.[73] Also, these channel networks allowed for a diffusive transport of the toxic waste products away from the cell. In the second cell type traps we investigated the same well design used by Dr. Luke P Lee where a continuous flow of fresh media holds the cells in place within the a hydrodynamic shaped cell trap.

To make the cell culturing easier an automated and portable cell culture chamber was designed, built, and tested that could either add fresh media continuously to the Jurkat cells or batch feed them. In this self contained system, the cells could be observed continuously without the risk of contamination.

## 4.2 Experimental

### *4.2.1 Chemicals*

Jurkat Clone E6-1 (lymphoblast) was purchased from the American Type Culture Collection (Manassas, VA). Cell media RPMI-1640, Phosphate buffered saline and Isopropanol was obtained from Fisher (Pittsburg, PA). SYTO16 was obtained from Invitrogen (Carlsbad, CA). Negative photoresist SU-8 2035 and 453 Microposit Developer was obtained from MicroChem Corp (Newton MA). Poly(dimethylsiloxane) was obtained from Sylgard®184 Dow Corning (Midland MI). Positive photoresist AZ P4620 and developer AK400 were obtained by AZ Electronics (Sommerville, NJ). Distilled deionized water was obtained from Barnstead Ultra pure Water System (Dubuque, IA) and filtered with a 0.45 µm Millex®-LCR syringe driven filter (Millipore Cooperation, Bedford, MA). Argon gas was obtained from Linweld (Manhattan, KS). All the chemicals were used as received.

### *4.2.2 Cell Culture Device Fabrication*

The procedure for device fabrication was discussed previously in Chapter 3.

### *4.2.3 Cell Line and Culturing Methods*

All the information on the cell line and culturing methods are discussed in Chapter 3.

### *4.2.4 Cell Imaging*

A Roper Scientific CCD camera was used to image these cells (Princeton Instrument Inc, Trenton NJ). A Nikon Eclipse TE2000E microscope with an epilluminiation attachment (Melville, NY) incorporated with an epiliuminescence system with a 500 W Mercury arc lamp and blue and green filter cubes for the excitation of dye, was used to image fluorescently labeled cells. SYTO16 was used to label the cell nuclei in cells mitosis stage.

## 4.3 Result and Discussion

### *4.3.1 The Portable Cell Culture Chamber*

To improve the viability of cells cultured in microfluidic devices a novel portable cell culture chamber was designed and fabricated. This chamber made it easier to feed the cells continuously instead of having to add fresh media or a mixture of fluorescent viability labels to the cells every sixth hour as was needed in the cell experiments in Chapter 3. Also the cell culture device is within a closed controlled environment while culturing, instead of having to be transferred from the cell incubator to the laminar flow hood for loading of media and dyes and the moved further to the inverted microscope for imaging.

In order to successfully cultivate cells in such a device some specific criteria needed to be met. The chamber needed to supply a constant temperature of 37°C, supply oxygen and carbon dioxide, and provide fresh media to the cells through either batch or continuous feeding. The cell culture chamber design was based upon a portable culturing system developed in the lab of Dr. Stanley Kleis at the University of Houston Clear Lake,

TX. It was built by Tim Sobering and Dave Huddleston at the EDL at Kansas State University. The cell chamber (Fig 4.3) was constructed from a plastic container with the dimensions of 12 x 15 x 25 cm. A thermoelectric heater with a set-point of 37°C was integrated into the box in order to provide temperature control. A small Peristaltic pump from (Instech Laboratories Inc, Plymouth meeting, Model P625)) was used to transport fresh media with a fluid flow range of 0.6-1.2 μm/min. Highly purified 5% carbon dioxide in air was pumped at 5 psi into the chamber through a Fisher brand polymer. The pressure into the chamber was controlled by the gauge on the gas cylinder.

The PDMS device was sandwiched together by the Plexiglas® plates with dimensions reduced from 15x 10x 1 cm to 7x 5x 0.5 cm (Fig 4.1). These covers prevented pressure points over the PDMS that could collapse channels and prevent leakage. The new top cover has Upchurch® reservoirs which help the loading of solutions and cells.
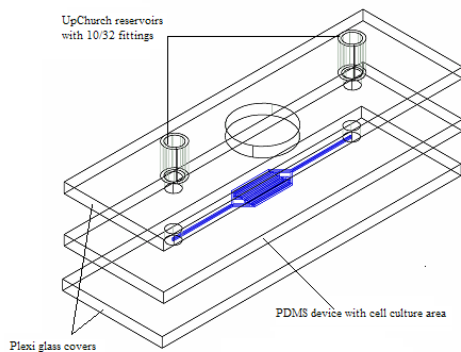


**Figure 0.1 - A schematic image of the cell culture device sandwiched between Plexiglas® covers.**

The device was loaded with solutions and cells on the laminar flow hood as described in Appendix A.8. The fresh media was added to a 2 mL sterile Eppendorf™ tube connected through sterile plastic tubing to the peristaltic pump. The pump then

transported the fresh media over the cells and to the outlet reservoir into a second sterile Eppendorf™ tube. After loading the Plexiglas® device was attached to the cell culture chamber.

The thickness of the Plexiglas® cover was important to ensure an even pressure distributed evenly over the PDMS device. This smaller Plexiglas®–PDMS sandwich was placed in the portable cell culture chamber. A small opening was removed from the bottom of the chamber was removed and the Plexiglas® device is placed over this opening for easy imaging using an inverted microscope (Fig 4.2A). This setup allowed for optical observation of the cells while remaining inside a heated environment with a continuous fresh media flow and allows for detection of cells loaded with fluorescent agents using a mercury arc lamp and blue and green filter cubes (Fig 4.2B).
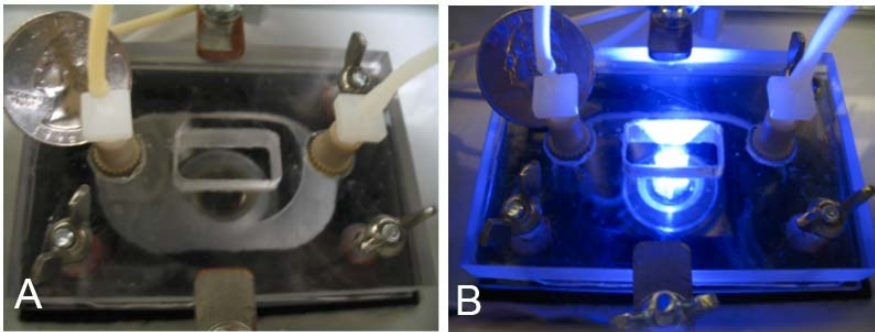


**Figure 0.2 - Inside the cell culture chamber the microfluidic device and be imaged by an inverted microscope with normal light (A) and with the excitation beam of 488 nm (B).**
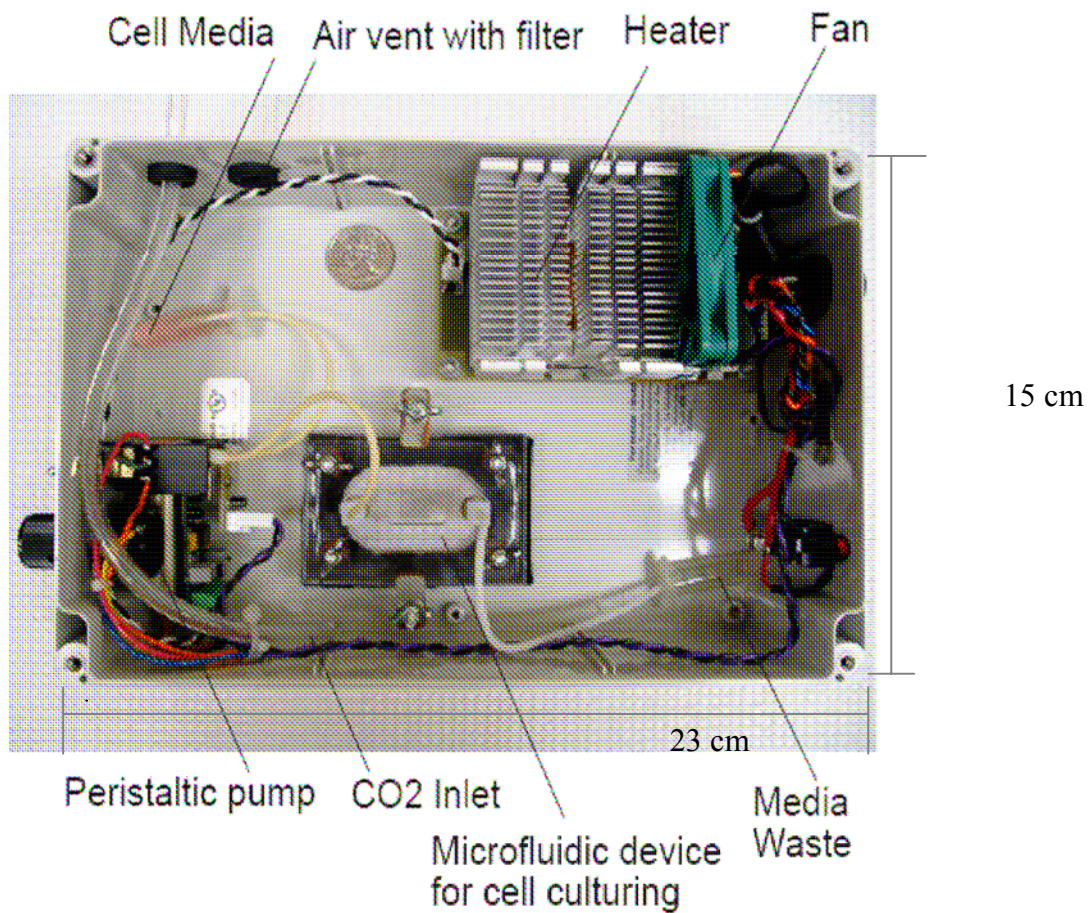
**Figure 0.3 - Top-down view of the components of the portable cell chamber.**

The cell culture chamber was started 10 min prior to the addition of cell culture device, this allowed the chamber to reach the optimum temperature of 37°C and a sufficient level of air with carbon dioxide, before the PDMS device with the cells were installed. After the chamber was assembled it was placed on the inverted microscope Nikon Eclipse TE2000E microscope with an epillumination attachment (Melville, NY) (Fig 4.4). The computer to the left in Fig 4.4 of the cell culture chamber was used to

collect images of the cells using a Roper Scientific CCD camera (Princeton Instrument
Inc, Trenton NJ)
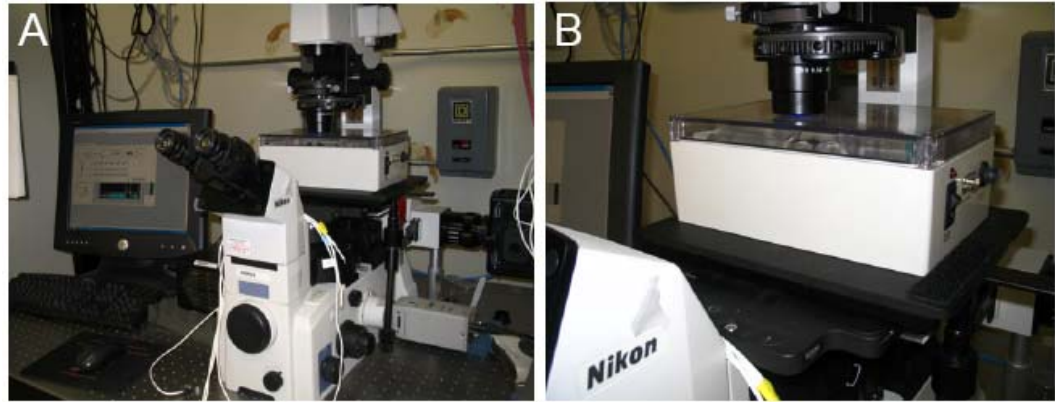


**Figure 0.4 - The portable cell culture chamber on the inverted microscope. A. The
computer to the left controlled the CCD camera. B Close up on the chamber and
microscope condenser.**

## *4.3.2 Fabrication and Results of Circular Cell Traps*

In order to build new cell traps able to hold just one cell at a time, the cell
diameter was measured. An aliquot of Jurkat cells was retrieved from a cell culture flask
cultured in the $CO_2$ incubator. The sample was mixed and a droplet was placed inside a
small Petri dish. The Petri dish kept the cells in an enclosed environment to prevent
evaporation while the cells were imaged. A microscope (Nikon Instrument Inc, Melville,
NY) was used to image the cells. The computer program Act-2 was used to capture
images and measure the diameter of the cells. The cell diameter was measured for 270
cells. The result of the measurement is shown in Fig. 4.5. It showed that 5% of the cells
ranged between 7-9 μm, while the majority 83% of the cells ranged in the size between 9-
13 μm and finally 3% of the cells ranged between 13-16 μm.
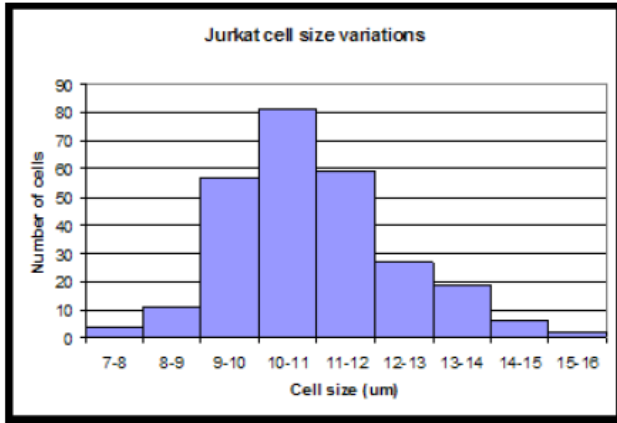
**Figure 0.5 - Measurements of the average Jurkat cell size (n = 270).**

Using this result we designed our cell array traps to be ~ 13 μm in diameter so that they would be able to hold only one Jurkat cell at a time. This size should be large enough to trap one cell on average, but as the cell divides into two daughter cells one of the cells should be pushed into the microfluidic channel and be transported for single cell analysis. Three out of the 4 patterns shown in Fig. 4.6 have narrow interconnecting channels with a channel width of 2 μm. These channels were added to promote cell to cell signaling between the cells after some of our initial culturing attempts resulted in very low cell viability. Four designs were made: The first pattern, had circular traps with a diameter of 13 μm (Fig 4.6A). The second pattern, the 13 μm traps with connecting channels with a width of 2 μm (Fig. 4.6B). The third pattern, has the 13 μm traps with connecting channels in a vertical direction (Fig 4.6C). The fourth pattern, has 13 μm traps with 2 μm wide signaling channels in all four directions of the well (Fig. 4.6D).
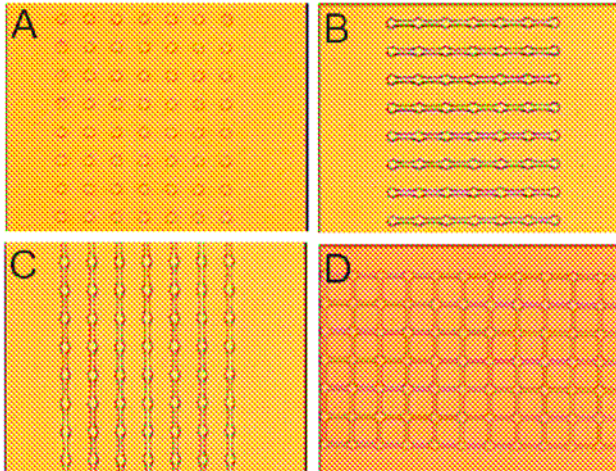
**Figure 0.6 - Four designs for the circular cell traps.**

Initial attempts to load the cells into the isolated 13 μm diameter wells proved to be problematic. Cell cultures of both low (4) and high (35) passage numbers were tried to see if the cell age changed the size of the cells, however, the wells did not fill efficiently. This is shown in Fig. 4.7 where only 6 out of 20 cells were filled with cells. The spinning time on the motorized hamster wheel was extended from 5 min to 12 min, however the cells still could not be forced into these wells. As seen in Fig 4.7 there should be enough space inside the well for cells, the reason might be that these wells were too shallow. The depths of these wells were 10 μm, which should be sufficient to hold a cell, however the experiment showed the opposite. Deeper circular traps were not fabricated, because at this point we had learnt that cell viability was increased when the cell was in a less confined environment.
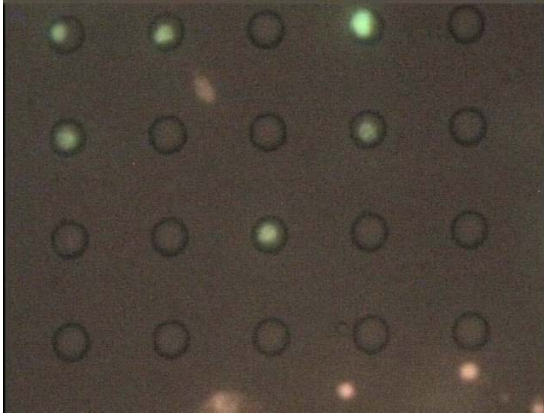
**Figure 0.7 - Single cells inside the 13 μm cell trap, the SYTO16 labeled cells (green) are alive and the Propidium Iodide labeled cells (pink) are dead.**

The same issue could be seen in the cell loading into the patterns with vertical or horizontal interconnecting channels. Even though the cells should have been able to fit inside the wells, this was not the case. Again the assumption was that these wells were to shallow, which prevented the cells for remaining inside the wells. However, the fourth pattern with the interconnecting channels did show some promise, as shown in Fig. 4.8.
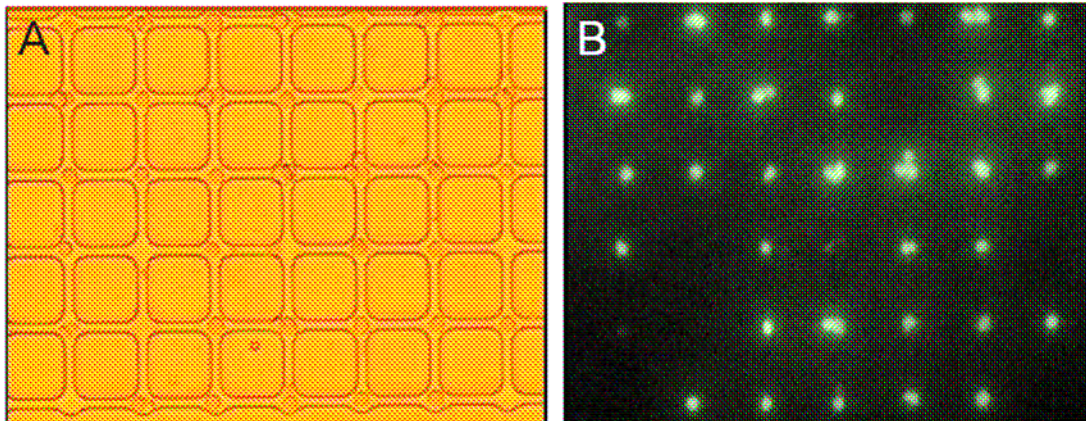


**Figure 0.8 - Cells labeled with SYTO 16. A. In light field and B. In dark field**

This is because the connecting channels make the inside of the cavity larger, due to the fact that this area was subjected to excess light during photolithography. The dimensions on the photomask for the interconnecting channels were 2 µm, but as seen in Fig. 4.8 the diameter of these channels appears to be 8 µm, which lead to unwanted cells in these channels. It was noticed that the wells contained more than one cell per well. This was reduced by excess washing with pre-warmed PBS to remove the excess cells, but the issue remained. The filling rate after loading of these traps was $19 \pm 2.8\%$ (n= 3), because the cell trap was too shallow which caused the cell to float away. Unfortunately, the cell viability of the cells that were trapped decreased rapidly and after 12 h it was 0% (n = 3).

### *4.3.3 Fabrication and Results of the Hydrodynamic Shaped Cell Traps*

In an effort to improve the cell traps we adopted a design similar to that recently published by the group of Luke P. Lee et al. (2006) [50]. The difference between the Lee group designs and ours is that the Lee group used a glass-PDMS hybrid device while we worked on a device made only from PDMS. The cell traps in this array have a concave shape for holding individual cells (Fig 4.9). The cells in this design have to be actively held in the traps by a constant influx of fresh media into the cell array.
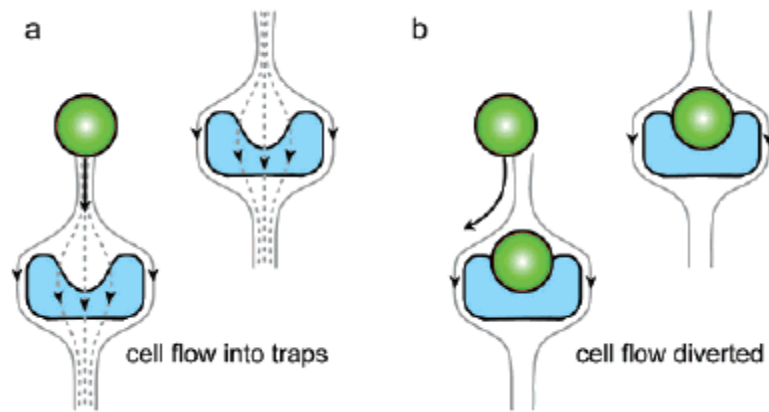
**Figure 0.9 - Hydrodynamic shaped cell traps designed by the Lee group.[50]**

These traps were designed to ensure that only one cell is cultured per trap. Two designs of traps were designed with the inner cavity size being 10 μm or 20 μm using AutoCAD LT 2006 from Thompson Learning (Albany, NY). The designs were electronically sent the Photoplot Store (Colorado Springs, CO) for fabrication. Photolithography and pattern transfer was used to fabricate a master mold as described in section 1.3.2. The fabrication of these traps, however, was slightly different from the fabrication of the cubic shaped traps in Chapter 3 it used a negative photoresist for its master mold fabrication. For the fabrication of the hydrodynamic shaped traps a positive photoresist was used, instead of fabricating an elevated master mold, positive photoresist made indents in the master mold. As the PDMS was poured on the master mold the polymer sinks into these small cavities in the master mold. After the polymer has cured the surface will have elevated cell traps. It should be noted that the photomasks used with a positive photoresist needs to be different from when a negative photoresist is used. When using a positive photoresist, the mask needs to be mostly transparent with an

opaque design. This is the opposite for the photomask used for a negative photoresist, where the majority of the mask is opaque and the channels are transparent.
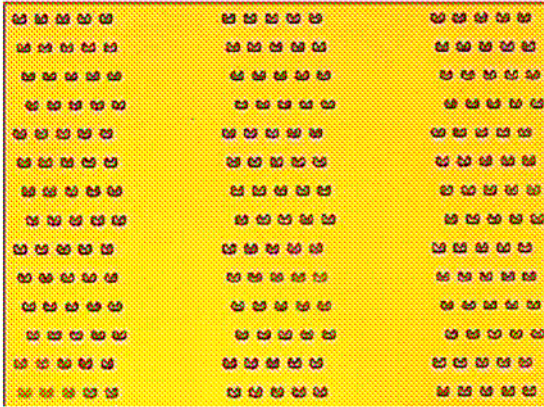


**Figure 0.10 - The master mold for fabrication of the C-shaped traps.**

We attempted to load cells in both the 10 and 20 μm cavities. The 10 μm cavity was most efficient for capturing single cells. When the cavity size was increased to 20 μm, many of the traps contained more than one cell. The cell traps shown in Fig 4.11 had a inner cavity size of 10 μm and a height of 10μm, while the channel network had a height of 13 μm. The short distance of 3 μm between the trap and channel was enough to allow solution not only to pass around but also under the cell traps. This 3 μm gap however, was to small for cells to pass under.
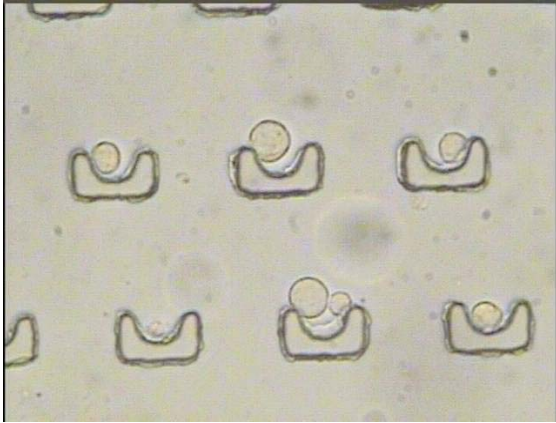
**Figure 0.11 - Jurkat cells in the C-shaped traps.**

It was very challenging to keep air bubbles out of the channel network over time. The air bubbles could have been generated by air pockets in the tubing or an air leakage in the connections. Another issue was preventing the PDMS channels from collapsing and cutting off flow in the channels. To ensure an even pressure over the cell culture area in an attempt to prevent the channels from collapsing, the top Plexiglas® plate thickness was increased from 0.5 cm to 1.25 cm. This decreased the propensity of the channels from collapsing. The improvements on the Plexiglas® design and the design of the hydrodynamic shaped traps resulted in an improved filling. The filling rate after loading of these traps was $95 \pm 3.5\%$ (n = 3). This was a significant improvement compared to the previous designs. Once trapped the cells were kept in place using a continuous flow of media at a fluid flow of 1.5 µL /min. The cell viability after 12 hours on this device was unfortunately was only $29 \pm 41\%$ (n = 3). The large standard deviation was a result of two experiments with high cell viability and one experiment with low cell viability. In these experiments it was found that the dynamic culturing method has advantages as constant addition of fresh media and dilution of waste products. It also has challenges

which lower the cell viability, due to air entering into the channel network which creates air pockets in the channel and dilutions of important cell signaling between the cells. With further optimization of the flow rate and improved connections between the pump and device this device has potential for culturing of single cells.

## 4.4 Conclusion

The results from Chapter 3 led to the conclusions that 1) the sizes of the cell traps needed to be reduced to hold only one cell at the time and 2) the addition of media over the cells needed to be more efficient and less likely to introduce contamination.

In this chapter two new cell traps were designed, fabricated and tested. The circular cell traps consisted of wells with diameters of 13 μm. However, over time it was noticed that the cells would not stay inside the circular shaped traps and the few that did stay inside the wells dried out after 12 h of culturing the cells. We also added interconnecting channels to these circular wells in the hope that this would promote cell growth. However after 12 h of culturing the all of the cells had died. The filling rate after loading of these traps was $19 \pm 2.8\%$ (n = 3). This might have been the result of the cell traps being to shallow.

A hydrodynamic shaped trap designed in the Luke P. Lee's group was tested. In these traps the cells were held in place by a media fluid flow of 1.5 μL /min. The advantage of this design is that the cell was constantly in the flow of fresh media and it allows for paracrine signaling. The filling rate after the loading of these traps was $95 \pm 3.5\%$ (n = 3). The cell viability after 12 h was $29 \pm 41\%$ (n = 3). The low viability in this chapter in comparison to chapter 3, are due to the different environments in the experiment. Here the media was added continuously, which has advantages as constant addition of fresh media and dilution of waste products. However this can also be challenges such as air leaking into the channel network which creates air pockets in the

channel and dilutions of important cell signaling between the cells. With further optimization, including optimizing the flow rate of media that sufficiently adds fresh media without diluting the cell signaling substances, these cell culture traps have the potential to be used for long-term culturing of individual cells.

In this chapter we also designed, built and tested an automated and portable cell culture chamber. In previous experiments the cell culture device was placed in the $CO_2$ incubator, then transferred to the laminar flow hood for loading of fresh media and dyes for cell viability testing and imaged on the inverted microscope. The cell viability was determined after 500 cells had been counted, which means that the microfluidic cell culturing device was at room temperature for at least 20 min per viability testing. The transfer of the device around the laboratory along with the replacement of the media and the addition of the viability fluorophores increased the risk for contamination. The portable cell culturing device developed in this chapter had an integrated a peristaltic pump for continuous media replacement, a thermoelectric heater, inlets for highly purified oxygen-carbon dioxide and Plexiglas® covers with Upchurch reservoirs for easy loading of solutions and cells should reduce the contamination potential in the future microfluidic cell culturing experiments. The advantage of this chamber was that the cells were less exposed to the risk of contamination and confined in a heated environment while cultured, labeled and counted for cell viability.

# CHAPTER 5 - ELECTROKINETIC INJECTIONS AND SEPARATIONS FROM A HYDRODYNAMIC FOCUSING STREAM

## 5.1 Introduction

The objective of this chapter was to investigate how to bring an sample to an intersection in a microfluidic device without exposing it to an electric field, and then to inject and separate the sample components. Such a system would have great potential in the analysis of single cells. Cells are very sensitive to electric fields.[53] Exposing a cell to an electric field prior to the actual analysis can perturb the results significantly. Therefore, a method is needed to transport the cells to an intersection where the cells can be rapidly lysed and the cells contents can be injected into a channel for electrophoretic separation. This system incorporating both hydrodynamic and electrokinetic flows can be designed as discussed below. The generation of hydrodynamic flows, however, can lead to excess band broadening[74] during the electrokinetic separation, therefore, the device has to be designed in such a way that the excess band broadening from the hydrodynamic flow is minimized. To evaluate the effectiveness of the design on reducing the band broadening effects of the hydrodynamic flow, the broadening of analyte bands was measured as the analyte migrated down the separation channel.

Minimizing analyte dispersion is important to ensure the fast and best separations possible. There are many sources of possible dispersion for an analyte during a separation. These sources can be measured and quantified as explained below. Factors

that can affect quality of separations are peak variance due to injection, detection, parabolic flow, joule heating, sample adsorption, and electrodispersion among others. All these contributions of band broadening add up to generate the total spatial peak variance ($\sigma^2$). All of these sources are stochastic in nature and so all will generate bands that are Gaussian shaped. Because of this and that the sources are nominally independent upon one another, they generally tend to be additive. To determine the contribution of time dependent analyte band broadening factors the spatial peak variance ($\sigma^2$) is plotted as a function of migration time ($t$). The slope of the straight line contains all of the band broadening sources that are dependent on time, factors such as longitudinal diffusion and parabolic flow. For a diffusion limited systems, the slope of the linear regression divided by 2 is equal to the diffusion coefficient ($D$) under the assumption of the Einstein-Smoluchowski equation:

$$\sigma^2 = 2Dt \qquad \text{(E5.1)}$$

The diffusion coefficient is dependent on the mean velocity flow ($R$), temperature ($T$) and the frictional force ($f$) according to equation E5.2:

$$D = \frac{RT}{f} \qquad \text{(E5.2)}$$

In order to find the experimental value for $y_{int}$ , the peak variance is plotted as a function of migration time (Fig 5.1). The y-intercept ($y_{int}$) of the straight line is the sum of the constant sources of band broadening due to injection ($\sigma^2_{inj}$) and detection ($\sigma^2_{det}$).

$$y_{int} = \sigma^2_{inj} + \sigma^2_{det} \qquad \text{(E5.3)}$$

The peak variance due to the detection window can be determined from the size of the spatial filter (800 µm) divided by the objective magnification. This contribution is

small compared to the contribution of the injection plug length, therefore, this factor can generally be disregarded.
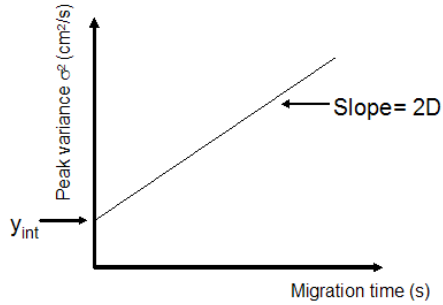


**Figure 0.1. - The peak variance as a function of migration time.**

The peak variance due to injection ($\sigma^2_{inj}$) can be used for calculation of the injection length ($l_{inj}^2$) from equation E.5.4.

$$\sigma^2_{inj} = \frac{l_{inj}^2}{12} \qquad \text{(E5.4)}$$

In this experiment there could be contributions to peak variance due to the use of parabolic flow. The peak variance because of parabolic flow is dependent on the mean velocity flow from the parabolic flow ($u_p$), channel depth ($d$), migration time ($t$) and diffusion coefficient ($D$) as seen in equation E5.5.

$$\sigma^2_{para} = \frac{4u_p^2 d^2 t}{105D} \qquad \text{(E5.5)}$$

## 5.2 Experimental Section

### 5.2.1 Chemicals

Acetone, dimethylsulfoxide (DMSO), methanol, sodium bicarbonate, sodium borate, sodium hydroxide were all obtained from Fisher (Pittsburg, PA). Amino acids

79

proline, serine and arginine were obtained from Biomedicals Inc. (Aurora, OH).

Fluorescein-5-isothiocyanate (FITC) and calcein AM was obtained from Invitrogen

(Carlsbad, CA). Double distilled water was obtained from Barnstead Ultra pure Water

System (Dubuque, IA) and filtered with a 0.45 μm Millex®-LCR syringe driven filter

(Millipore Cooperation, Bedford, MA). Epoxy 353ND was obtained from Epoxy

Technology (Billerica, MA). All the chemicals were used as received without any further

purification.

### 5.2.2 Single-Point Detection System

The Single-point detection system was described in section 1.4.1.

### 5.2.3 Imaging Injections

Nikon Eclipse TE2000E microscope with an epilluminiation attachment

(Melville, NY) was used to image the injections. The single throw double pole (STDP)

was built by the EDL at KSU. The high voltage power supply was built in-house.

### 5.2.4 Microfluidic Device Fabrication

The glass microfluidic devices were fabricated according to the procedure

discussed in section 1.3.1. The dimensions of the microfluidic device used in these

experiments are shown in Fig. 5.2, all measurements are listed in centimeters.

Calculations of the fluid resistance are the reason why the majority of channels have a

channel width of 25 μm and sections by the reservoirs with a channel width of 90 μm.

The channel depth of the devices was 10 μm and 20 μm. The 10 μm channels

were to used for separations of fluids for comparison of previously reported data

diffusion coefficient.[75, 76] The devices used for cells were etched to 20 μm, because the single Jurkat cell has an approximate diameter of 13 μm.
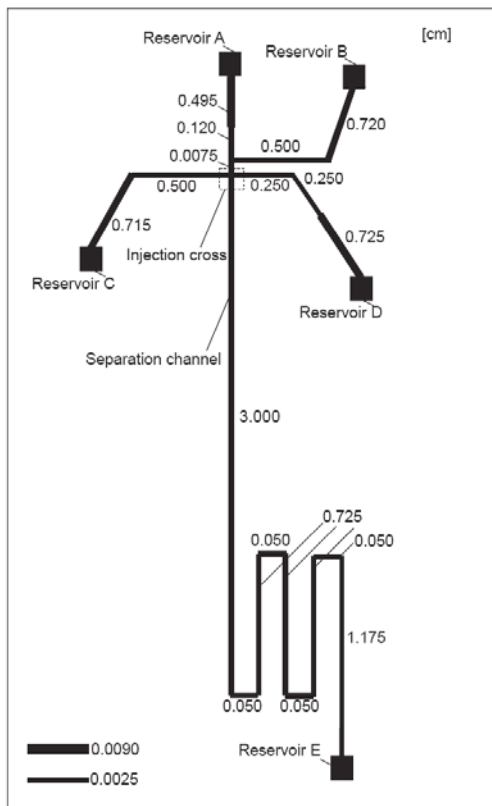


**Figure 0.2 - Schematic of the microfluidic device used for the amino acid separations.**

### 5.2.5 Fluidic Resistance

To reduce the contributions of band broadening due to the parabolic flow the fluidic resistance was increased in the separation channel. This increase in fluid resistance in the separation channel prevents the fluid that is being transported to reservoir D from being pulled back into the separation channel. It is extremely important to minimize this backflow, since it can cause the injection plug to broaden as it migrate down the separation channel which will lead to a non-Gaussian shaped electrogram.

The microfluidic devices with a channel depth of 10 μm have a design with a 20x higher fluid flow resistance in the separation channel compared to the channel between reservoir A and the intersection (Fig 5.2). The microfluidic devices with a channel depth of 20 μm have a design with a 50x higher fluid flow resistance in the separation channel compared to the channel between reservoir A and the intersection. The equations for fluidic resistance have been discussed in section 1.4.4.

### *5.2.6 Single Throw Double Pole Switch (STDP)*

The STDP is based on the same principle an electromagnet, simply made from a coil and metal. As a current is sent through the coil it energizes an electromagnetic field that can switch high voltages on and off.[77, 78]

The injection was initiated by the computer program LabView to send 5 V from the high voltage (HV) power supply to the coil which energizes a magnet within the STDP. This switches a flexible wire between the connections Normally Closed (NC) and Normally Opened (NO). When the electric circuit is closed the high voltage goes through the NC electrode while the high voltage in the NO is floating. Once the STDP is initiated by LabVIEW the voltages goes through NO while the high voltage in NC were floating. After the injection time has passed the voltages goes back to the original setting.

### *5.2.7 Diffusion Coefficient Calculations*

The diffusion coefficients were calculated from FITC-labeled amino acids detected at five distances: 1.016, 1.270, 1.524, 1.778 and 2.032 cm in the separation channel. These exact distances were measured using the micrometer on the single point system. The peak amplitude does decrease as the separation length increases, because as

the analyte band travels down the separation channel it get broader and does not have the same intensity, hence the amplitude decreases. The peak amplitude decrease of FITC-labeled proline is shown in Fig 5.3. To show that the data was reproducible each separation was run five consecutive times for each detection length.
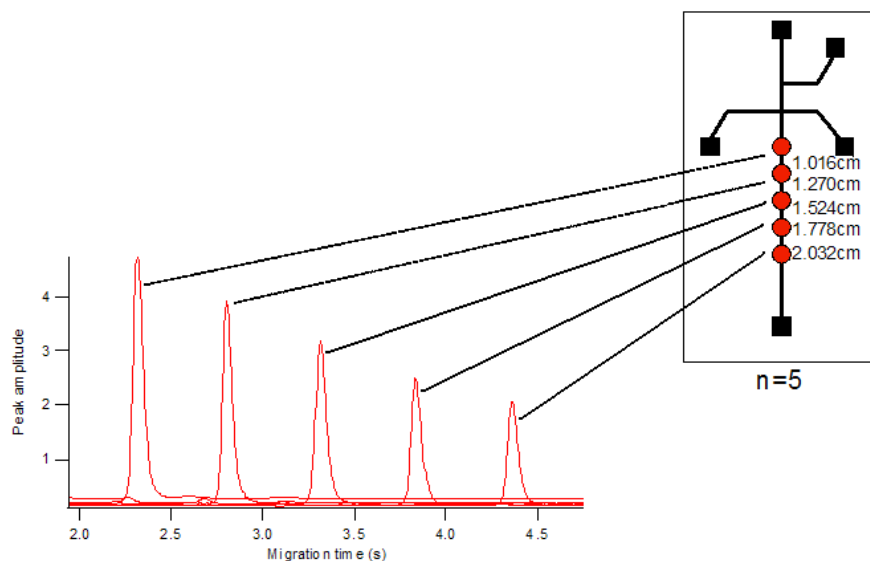


**Figure 0.3 - Electropherograms of FITC labeled proline at the detection distances 1.016 cm, 1.270 cm, 1.524 cm, 1.778 cm, 2.032 cm. (n=5)**

The temporal peak variances of the analytes were calculated by fitting them to Gaussian equations[79] using the IGOR data analysis program. The temporal peak variance ($\sigma_t$) was converted into spatial peak variance ($\sigma_{sp}$). The spatial peak variance was plotted as a function of the migration time ($t$) as shown in Fig 5.4. The data points were fitted to a linear regression and the slope of the straight line was equal to the diffusion coefficient divided by 2, as discussed in section 5.1.
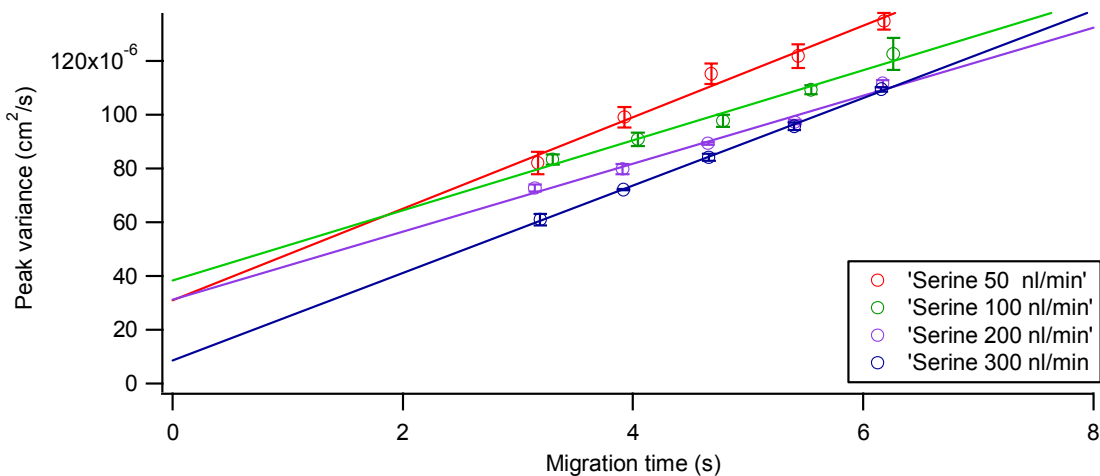
**Figure 0.4 - Peak variance over migrations time for FITC-labeled serine on a device with a channel depth of 10 $\mu$m (n = 5)**

## 5.3 Result and Discussion

### *5.3.1 Injections of Amino Acids*

The gated injections were made via the hydrodynamic fluid stream of analyte into the separation channel. The sample was transferred from reservoir A (Fig. 5.2) to the reservoir D which was connected to the syringe pump. High voltage electrodes were placed into reservoir B and reservoir C, a ground wire was connected to the reservoir E. The high voltages setup is shown in Fig. 5.5. High voltage 1 (HV1) was send a potential by the LabView program, which created an electroosmotic flow from reservoir C to reservoir D (Fig. 5.2). This prohibited leakage of the analyte into the separation channel. Meanwhile the voltage in high voltage 2 (HV2) was floated (Fig 5.5A). The injection was initiated by the LabView program sending a low voltage to the single throw double pole (STDP) relay. The STDP switched the high voltage 1 to be floated, while the potential was applied at high voltage 2. This created an electroosmotic flow from reservoir B to

84

reservoir E. As the result of the electroosmotic flow, a small amount of analyte was injected into the separation channel (Fig 5.5B). After injection time of 20 ms had passed the STDP was switched back into its original setting (Fig 5.5C).
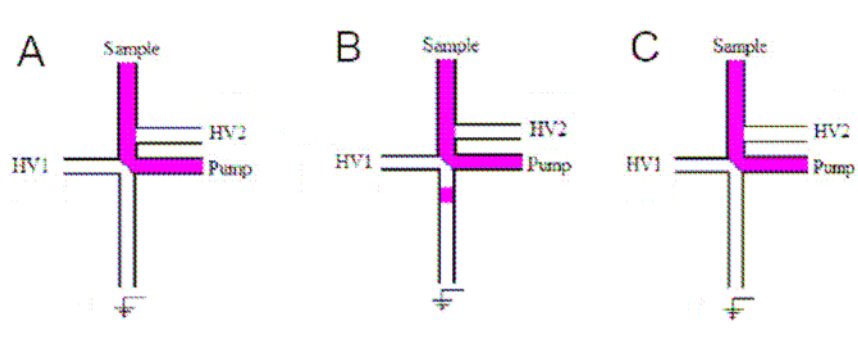


**Figure 0.5 - Illustrates the gated injection from a hydrodynamic focused stream.**

Fig. 5.6 shows real images of FITC-labeled proline during the manual injection process. The injection plugs in these images are longer those initiated by the LabVIEW program, because of human limitations of flipping a switch back and forth. The channel design used for this injection is shown in Fig. 5.1. The sample was pulled from reservoir A to reservoir D (Fig 5.6A). After injection initiation an analyte plug was formed at the intersection (Fig 5.6B). The analyte plug was injected and transported down the separation channel (Fig 5.6C-F).
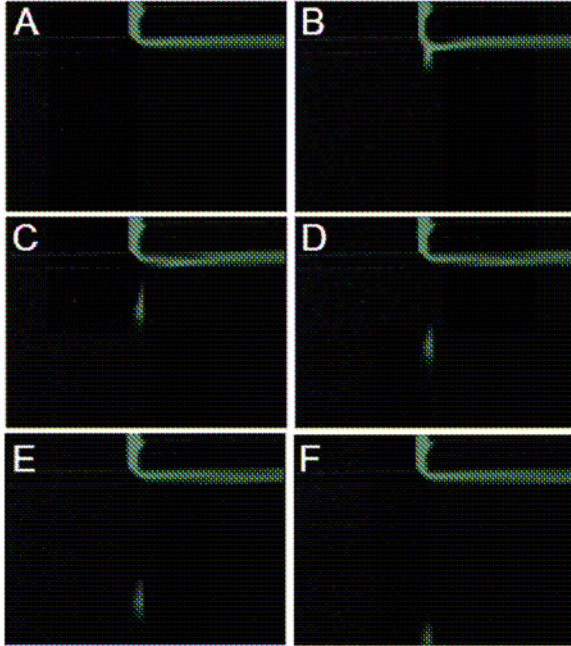
**Figure 0.6 - Real-images illustrating a manually made injection of FITC-labeled proline.**

## *5.3.2 Results of the Diffusion Coefficient Study*

The diffusion coefficients were calculated for FITC-labeled arginine, proline and serine with channel depth of 10 μm and 20 μm at flow rates of 50, 100, 200 and 300 nL/min. The diffusion coefficient values were corrected for the temperature, from 25 °C to the actual temperature of 21.1 °C when the data was collected.[75, 80, 81]

$$D_{25°C} = D_{X°C} \frac{T_{25°C} \eta_{X°C}}{T_{X°C} \eta_{25°C}} \qquad (E5.7)$$

The results of the diffusion coefficients calculations for Arginine, Proline and Serine at the channel depth of 10 μm and 20 μm were plotted as a function of the flow rates (Fig. 5.7) In this graph the diffusion coefficients range in 4 x$10^{-6}$ to 8 x$10^{-6}$ cm$^2$/s, which is in the range of previously reported diffusion coefficient values for amino acids (5 x$10^{-6}$ cm$^2$/s).[81, 82] The exception was arginine on a 20 μm deep device that at 50

nL/min has a slightly higher diffusion coefficient, which indicates that the bands were being broadened slightly by a parabolic flow.
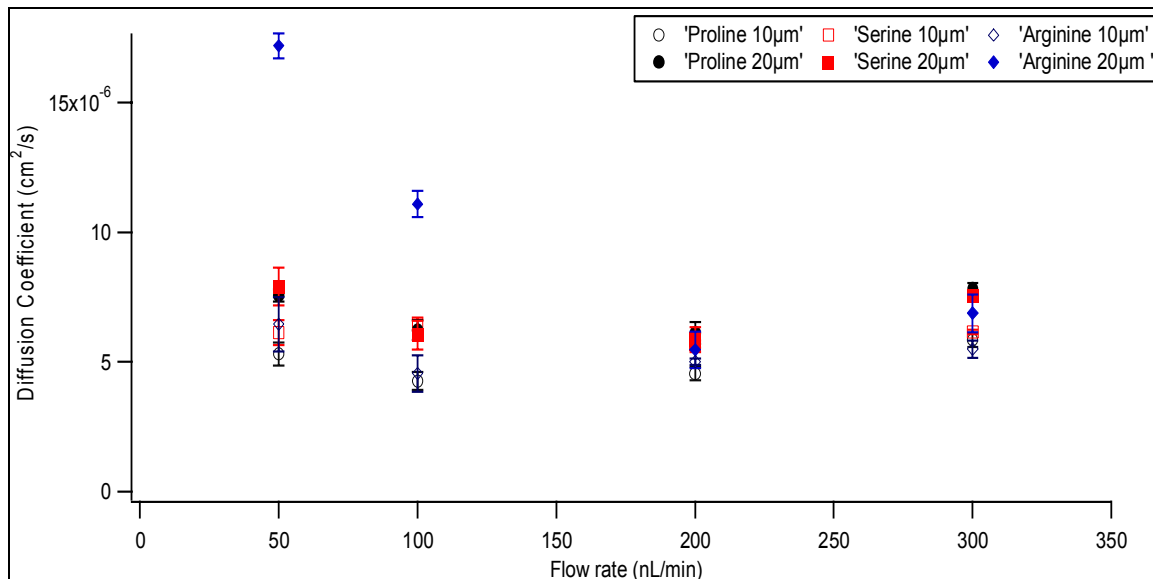


**Figure 0.7 - Diffusion coefficient as a function of flow rate for FITC-labeled arginine, proline and serine on devices with a channel depth of 10 μm and 20 μm. (n=5)**

The separation efficiencies were calculated from the arginine, proline and serine peaks in the electropherograms. The IGOR software was used to calculate the base width and migration time for each amino acid (n = 5). The resulting efficiency ranges from 17,000-56,000 theoretical plates for the three amino acids. The overall separation efficiencies were consistent over the increasing flow rates (Fig. 5.8). If the flow rate significantly influenced the separations, an overall decrease in separation efficiency would have been observed, because the peak variance due to the parabolic flow ($\sigma_p^2$) would increase (according to the E5.8). The separation efficiency is therefore expressed

as the separation length ($l$) over the peak variances due to diffusion ($\sigma_d^2$) and parabolic

flow ($\sigma_p^2$).

$$N = \frac{l^2}{\sigma_d^2 + \sigma_p^2} \qquad \text{(E5.8)}$$
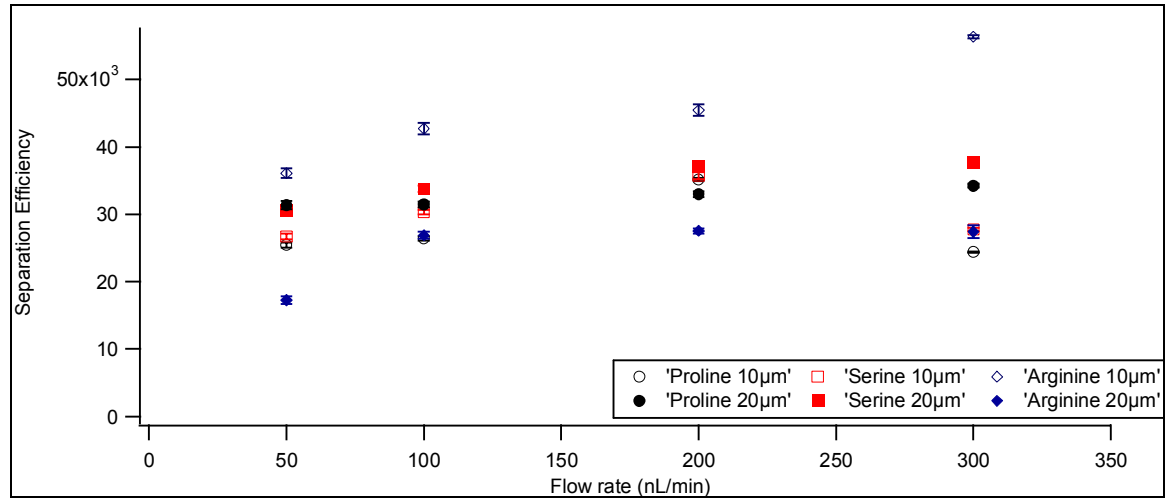


**Figure 0.8 - Separation efficiency as a function over the flow rate for FITC labeled arginine, proline and serine separations on 10 μm and 20 μm deep devices. (n = 5)**

To investigate how the injection length varies with the different flow rates the y-intercept of the linear regression was used to calculate the injection length, according to equation E5.3. The injection lengths were plotted as a function over flow rates as shown in Fig 5.9. This graph shows a decrease in the injection length as the flow rates increase. This is expected since as the flow rate increased there was a smaller amount of analyte at the intersection to be injected into the separation channel. It should be noted that the data points (n = 5) in Fig. 5.9 are equipped with error bars, but they are not visible in this graph.
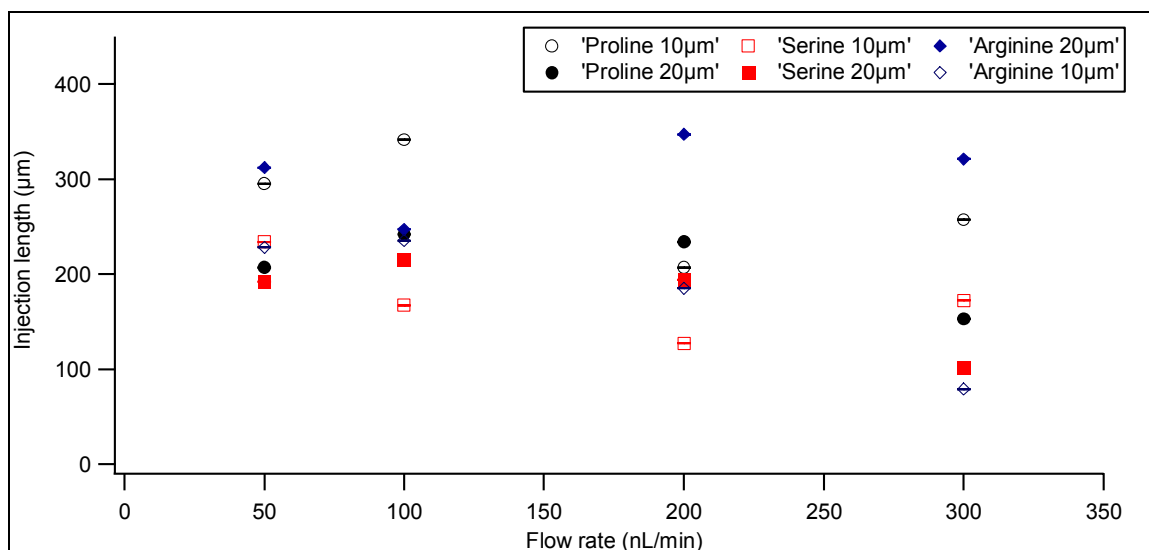
**Figure 0.9 - Injection lengths over the different flow rates for FITC labeled arginine, proline and serine for separations on 10 μm and 20 μm deep devices. (n=5)**

All the results from calculations of diffusion coefficient, separation efficiency, injection length and $R^2$ values are concluded in Table 2. The Figures 5.7, 5.8 and 5.9 are based on the values of Table 2.

**Table 2. - The conclusion table of diffusion coefficients, separation efficiencies, injection lengths and R$^2$-values for all the separations on 10 μm and 20 μm deep devices.**

| PV17, 10 μm, Fluid resistance: 20x | | | | | |
|---|---|---|---|---|---|
| Amino acid | Flow Rate | Diffusion Coefficient | Efficiency | Injection Length | R$^2$ value |
| | (nL/min) | (cm$^2$/s) | | (μm) | |
| Arginine | 50 | 6.46E-06 | 36,100 | 228 | 0.9672 |
| Arginine | 100 | 4.56E-06 | 42,690 | 235 | 0.9713 |
| Arginine | 200 | 5.02E-06 | 45,400 | 185 | 0.9992 |
| Arginine | 300 | 5.50E-06 | 56,350 | 79 | 0.9951 |
| Proline | 50 | 5.31E-06 | 24,430 | 295 | 0.9908 |
| Proline | 100 | 4.26E-06 | 26,430 | 341 | 0.9914 |
| Proline | 200 | 4.55E-06 | 35,130 | 207 | 0.9957 |
| Proline | 300 | 5.85E-06 | 24,370 | 257 | 0.9970 |
| Serine | 50 | 6.13E-06 | 26,720 | 234 | 0.9922 |
| Serine | 100 | 6.47E-06 | 29,670 | 167 | 0.9980 |
| Serine | 200 | 5.68E-06 | 35,700 | 127 | 0.9993 |
| Serine | 300 | 6.16E-06 | 27,770 | 112 | 0.9997 |

| Amino acid | Flow Rate | Diffusion Coefficient | Efficiency | Injection Length | $R^2$ value |
|---|---|---|---|---|---|
| PV19, 20 µm, Fluid resistance: 50x | | | | | |
| | (nL/min) | (cm$^2$/s) | | (µm) | |
| Arginine | 50 | 1.72E-05 | 17,240 | 312 | 0.9904 |
| Arginine | 100 | 1.11E-05 | 26,890 | 247 | 0.9974 |
| Arginine | 200 | 5.48E-06 | 27,530 | 347 | 0.9798 |
| Arginine | 300 | 6.89E-06 | 27,410 | 321 | 0.9855 |
| Proline | 50 | 7.56E-06 | 31,350 | 207 | 0.9974 |
| Proline | 100 | 6.23E-06 | 31,440 | 242 | 0.9950 |
| Proline | 200 | 6.12E-06 | 33,000 | 234 | 0.9938 |
| Proline | 300 | 7.83E-06 | 34,250 | 153 | 0.9989 |
| Serine | 50 | 7.91E-06 | 30,650 | 192 | 0.9898 |
| Serine | 100 | 6.04E-06 | 33,800 | 215 | 0.9890 |
| Serine | 200 | 5.86E-06 | 37,050 | 194 | 0.9916 |
| Serine | 300 | 7.56E-06 | 37,750 | 101 | 0.9995 |

### 5.3.3 Testing the Injections with Fluorescent Beads

Fluorescent beads with a diameter of 10 µm were used as a model for cells. These beads were mixed in a 1:50 ratio in a 10 mM sodium borate with 10µM FITC added to help visualize the fluid flow. The beads were added to reservoir A (Fig 5.2) and transported at a flow rate of 100 µL /min, as shown in Fig. 5.7. The bead would follow the hydrodynamic flow from reservoir A to the reservoir D (Fig 5.7) when there were no attempts of an injection. In order to inject a bead to the separation channel the STDP switches the high voltages just as the bead approached the intersection, according to the injection principle discussed in section 5.3.1.
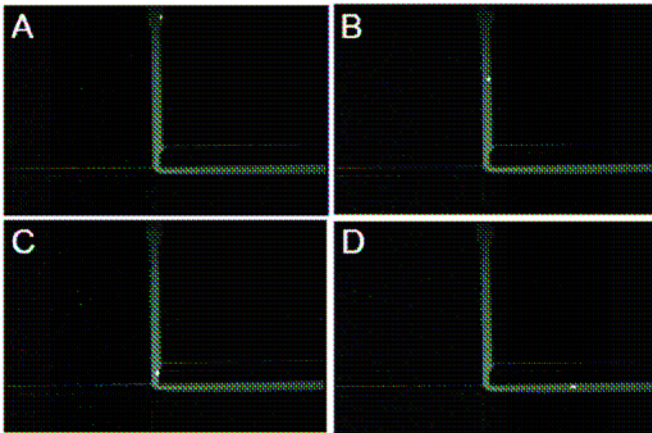


**Figure 0.10. - Images illustrating a fluorescent bead in a 10 µM FITC solution being transported by the hydrodynamic flow.**
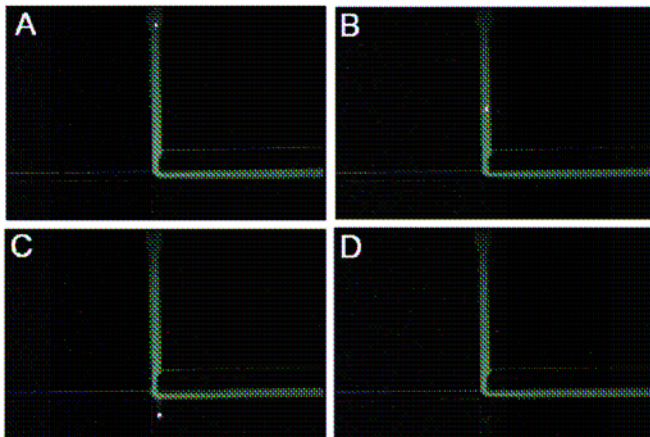
**Figure 0.11. - A series of images illustrating how a fluorescent bead in a 10 μM FITC solution is being injected in the separation channel.**

### 5.3.4 Results of the Initial Testing of Single Cell Lysis

The result from injections of amino acids indicates that separations could be performed without significant band broadening due to the parabolic flow. Therefore, cell lysates should be able to be injected without a significant loss of separation efficiency. Single cell lysis is necessary because even cells of the same type respond differently to the same external stimuli, as discussed in section 2.1.2. It is important to have a platform where a large population of cells can be tested using a rapid analysis technique. In this chapter we explore a simple system without valves for transportation and lysis single cells. The ultimate goal is to incorporate results from the single cell culturing (Chapter 4), label cells with a fluorescent tag and analyze them using the procedure explained in this chapter. Previously it has been reported, that cells need to be individually loaded with a fluorescent protein and then individually lysed before the cell lysate could be added to the

capillary to analyze the cell content[46] or that microfluidic valves have been used to hold fluid areas separated to perform single cell lysis.[83, 84]

In our experiment the cells were loaded in the sample reservoir A (Fig. 5.2) then transported into the intersection by hydrodynamic flow. As the cell approaches the injection cross (Fig 5.12A) the high voltages were switched through the STDP relay and the electric field disrupt the cell membrane. This caused the cellular content to leak out and the lysate was injected into the separation channel.

In order to successfully and completely lyse cells in a microfluidic device the cell must be exposed to high potential for long enough time to be effectively lysed. Previous results have shown that exposure to an electric field strength of 900 V/cm for <100 ms is sufficient to lyse the cell membrane. The initial results in Figure 5.12 shows that it is indeed possible to transport, lyse and inject cell lysate on a microfluidic device.
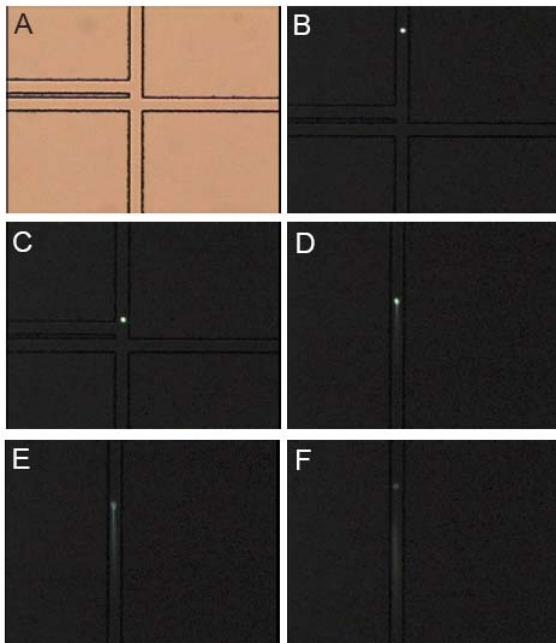
**Figure 0.12 - Images illustrating a calcein AM labeled cell approaching the intersection (Fig A-B), at the intersection where the high voltage was applied (Fig C) and after the cell membrane was disrupted and the cell content was released (Fig D-F).**

Naturally this experiment needs further optimization, the exact location where the cells need to be applied to the high electric voltages for complete cell lysis needs to be established.

To prevent cell debris from sticking to the channel wall, the microfluidic channels were flushed with Trypsin-EDTA for 1 min using a low vacuum flow prior to the cell loading. Normally, this solution is used to remove adhesion cells from the cell substrate as the EDTA removes the calcium ions.

## 5.4 Conclusion

In this chapter a novel injection method have been tested for fluids, particles and cells. The combination of a hydrodynamic stream and a gated injection were evaluated by the diffusion coefficient. The injections were tested by FITC labeled Arginine, Proline and Serine.

Separations have been performed on two types of devices. The first, used for amino acid had a channel depth of 10 μm and a 20x higher fluidic resistance in the separation channel. The second, used for particles and cells had a channel depth of and 20 μm and a 50x higher fluidic resistance in the separation channel. Separations were tested at flow rates of 50, 100, 200 and 300 nL/min. The resulting diffusion coefficients were in the close range of previously reported values, which indicate that this injection method should be amenable to separating the contents of lysed cells that are brought to the

injection intersection using a hydrodynamic flow. This device was initially tested with fluorescent beads with a diameter of 10 µm, to transport and inject them to the separation channel. In the end we started using the device for Jurkat cells. The Calcein AM labeled cells have been transported by a hydrodynamic flow in the microfluidic channels and lysed at the injection cross. The lysate was injected into the separation channel (Fig 5.12). The cell lysis does require further optimization to preventing cell debris from remaining in the microfluidic channels. These studies are of high importance for fundamental studies of biochemistry as well for the pharmaceutical science.

# Appendix 1- Fabrication of PDMS devices

## A.1 Fabrication of Master Mold for the Channel Network

Set the temperatures on the Fisher Scientific hot plates to 60°C and 95°C.

Use a Corning Glass slide 2x3" and clean it with Argon gas.

Use the Repeater® plus Pipette (Eppendorf™) to swirl SU-8 (2035) onto the glass slide.

From now on, protect the photoresist from light at all times. Place the glass slide in the

holder on the spin coater (Laurell Technology Corporation, Model WS-400A-6

NPP/LITE)

Select program G, programmed to spin at 570 rpm for 16 s and then 15 s at 600 rpm.

Start the spin coater by: make sure the lid is closed, open the gas tank, press the vacuum

button to initiate the vacuum and finally press start.

Pre-bake the photoresist, by placing the glass slide on the 60°C hot plate for 5 min,

transfer to the 95°C hot plate for 8 min and let the slide cool down for 7 min.

Move to the flood exposure system; place the slide inside the light protected area. Choose

the photomask needed for the master mold. Place the mask over the photoresist and lay a

¼'' thick Quartz glass slide on top of the photomask to prevent the mask from bending.

Expose the photoresist to the Ultra-violet Flood exposure Illumination system, (87000

Series) for 5.00 s.

Post bake the photoresist at 60°C for 1 min, then at 90°C for 5 min and finally let the plate cool for 3 min.

Place the glass slide in the SU-8 Developer, 453 Microposit Developer (Shipley) for 1 min.

Carefully rinse the surface with isopropanol.

Apply a gentle flow of Argon gas over the surface.

Then place the glass slide in the 80°C Lindberg/ Blue Mechanical Convection Oven for 10 min.

## A.2 Fabrication of Master Mold for the Hydrodynamic Shaped Traps

Use a 2 x3' glass slide clean it in a soap solution, rinse with double distilled water and dry in a 100°C oven.

Place the glass slide on the spin coater, start at 15s at 300 rpm, then increase to 1000 rpm for the next 16 s.

Pre-bake on a Fisher hot plates for 5 min at 65°C, 5 min at 90°C and let the glass slide cool down for 5 min.

Expose to UV-light for 4.3 s.

Post bake in the same way as pre-bake.

Place in the AZ200 developer for 3 min.

Wash the master mold with isopropanol.

Dry in the oven for 10 min.

# Appendix 2- Preparation of Amino Acids Labeled with Fluorescein-5-Isothiocyanate (FITC)

Start with a vial with 5 mg of fluorescent dye (FITC)

Add 1 mL DMSO to the vial. The concentrations will be of the 12.8 mM for FITC.

Prepare a 5 mM sample of the amino acid in 10 mL of sodium bicarbonate (150 mM at pH 9.)

Take 900 µL of the amino acid and add 100 µL of the fluorescent dye (prepared in step 1)

Place the Eppendorf™ tube on a Vortex and cover with Aluminum foil. Shake the sample for 4 h in room temperature.

Store in freezer until the sample is needed.

# Appendix 3- Suspension Cell Protocols

## A.3 Preparation of Penicillin and Streptomycin

Preparation a stock solution with the concentration of 0.1 g/mL. (Tube A) E.g. Tube A with 0.658 g of Penicillin will be added approx 6.6 mL HBSS buffer. Mix the sample to dissolve the Penicillin.

Make the solution of 0.02 g/mL. (Tube A1, A2, A3) Add 2 mL of the stock solution and 8 mL of HBSS to a new tube. Mix well before using in the next step.

To make the concentration 0.01 g/mL

(Tube A1.1, A1.2, A1.3, A2.1, A2.2, A2.3, A3.1, A3.2, A3.3)

Add 2.5 mL of the HBSS to a new tube and add 2.5 mL of the 0.02 g/mL solution. These samples do not have to be mixed if they will be placed in the freezer. However it is highly important to mix a sample well before adding it to a new media bottle.

## A.4 Preparation of New RPMI-1690 Media Bottle

Place and a culture flask and pipettes in the biological hood (3x 25 mL and 3x 5 mL) and expose with UV light for 10 min.

Preheat the Fetal Bovine Serum (FBS) in a water bath at 37°C for 30 min.

Defrost the Penicillin and Streptomycin in room temperature.

Wipe off the media bottle carefully (especially the top) with a Kimwipe® soaked in 70% ethanol outside the hood.

Wipe off the media bottle again inside the hood with Kimwipe® soaked in 70% ethanol.

After the Penicillin and Streptomycin have defrosted completely check to see that volume is 5 mL. Wipe the tubes off outside the hood.

Wipe off the Penicillin and Streptomycin inside the hood.

Wipe off the FBS outside the hood with big wipe with ethanol.

Wipe off the FBS inside the hood with a Kimwipe® with ethanol.

Start by preparing FBS. Mix the content five times using a 25 mL pipette.

Remove 25 mL FBS and add to the new media bottle. Then transfer another 25 mL FBS to the new media bottle.

Mix the Streptomycin (e.g. G1.3) three times and then add the solution to the new media bottle.

Mix the Penicillin (e.g. A.1.1) three times and then add the solution to the new media bottle.

Label the media bottle with the following information: month of arrival, opening date, initials, FBS, Penicillin and Streptomycin.

Place the media bottle in the yellow bag from ATCC and place in refrigerator. Label the outside of the bag with "Complete media".

The media needs to be tested before used for cell culturing. Place a test flask with 10 mL media in the incubator for 5-7 days. If there were no changes after the 5-7 days, the media is ok to use.

# A.5 Protocol for Resuscitation of Frozen Cell Line

(Written from combined information from Mälardalens University, Sigma Aldrich protocol and ATCC for Jurkat Clone E6)

The following material is needed to bring up 1 vial from the liquid Nitrogen dewar:

The night before experiment: prepare 2 tissue culture flasks with 5 mL media in each and place in the    incubator overnight. This allows for $CO_2$ to equilibrate to be reached in the media.

Place the following under UV light for the night: 10 mL (4), pipettes 2 mL (5), centrifuge tubes 15 mL (2), cell culturing flasks (2),

Preheat the water bath to $37\,^{\circ}C$.

Wipe off the media bottle one time outside the biological hood and once again inside the hood with a Kimwipe® soaked in 70% ethanol.

Label your new tissue culture flasks with cell line name, initials, date and content ratio of suspension to media.

Prepare two centrifuge tubes with 9 mL media in each. (One will be used only as a backup.)

Before opening the BioCane dewar the following safety equipment must be worn: lab coat, goggles, plastic gloves, face shield and cryogenic gloves.

Use forceps to retrieve the cryogenic vial from the liquid Nitrogen. Slowly take up the basket in the BioCane dewar, to reduce splashing of liquid Nitrogen.

Be really careful: The vial can explode!

Lower the vial in 37 $^o$C warm water bath. To reduce the risks of contamination keep the O-ring and cap of the vial above water level. Stand beside the hood and stir the vial in the water. The defrosting time should be about 2 min.

Remove the vial from the bath as soon as contents were thawed. Wipe of the vial with 70% ethanol and place in Class II Safety hood. From now on everything needs to be kept sterile.

Do not remove any of the safety equipment until the vial has been opened. Use a Kimwipe® soaked with 70% ethanol to hold around the vial and carefully loosen the cap slightly to open.

Close the vial again and place the vial in the biological hood. Remove the face-shield and cryogenic gloves.

Carefully transfer the 1 mL cells content to the "wash" media in the 15 mL centrifuge tube.

Centrifuge the cells at 800 rpm for 5 min. Clean the outside of the centrifuge tube with 70% ethanol before returning to the biological hood. Transfer the media flasks from the incubator to the biological hood.

After centrifugation remove the supernatant with a 10 mL pipette. "Shake up" the pellet (i.e. tap tube to loosen the pellet) and resuspend in 2 mL of media from the pre-equilibrated flasks.

Transfer the cell content to the flask with 5 mL $CO_2$ equilibrated media.

Label your cell culture flask with cell line name, initials, date and content ratio of suspension to media.

Incubate flask overnight.

Check after 24 h. Split into 2 flasks and feed both 5 mL of complete media. One set should be left alone on the top shelf of incubator for 2-3 days. The 2$^{nd}$ set should be placed on the lower shelf of incubator and counted daily to chart growth/viability. After splitting the "counting" flask it needs to be counted every day to make a cell growth graph. The resting flask should be left until it has yellow color, then calculate the ratio of alive and dead cells and split accordingly.

# A.6 Protocol for Feeding and Counting cells

Ensure that the following items are in close proximity: pipettes, waste bottle, Kimwipe®,

70% ethanol bottle and trash cane.

Transfer the media from refrigerator to incubator, warm to 37°C.

Sterilize the biological hood by exposing the surface to UV light for 30 min.

Clean the media bottle outside the biological hood using a Kimwipe® soaked in 70%

ethanol. Clean media bottle again inside hood with a Kimwipe® soaked in 70 % ethanol.

Loosen caps on media bottle and cell flasks.

Add 6 mL fresh media to a cell culture flask.

Transfer the cell culture flask from the incubator.

Add 2 mL cell suspension to the cell culture flask with 6 mL media.

Transfer the cell culture flask to the incubator for culturing.

Clean up bench area with EtOH. Clean pipettes and flasks with a 10 % Clorox® solution.

Prepare for cell counting, by taking a 1 mL sample from the cell culture flask.

To an Eppendorf tube add 5 drops of Trypan (blue) solution to the 5 drops of suspension.

Mix solution three times and fill up the two chambers of the Haemocytometer.

Calculate living cells (white) and dead cells (blue).

Calculate viability: (# living/ #total) x 100= [# %]

Calculate cells/ mL: #total x 1000 x 4 = [# cells/mL]

Calculate cells: (cells/mL) x 8 mL = [# cells]

Calculate viability/mL = viability/ # mL

## A.7 Protocol for Freeze back of cell suspension:

Remove the DMSO from the freezer.

Take out a sample of cells to calculate cell viability and viability/mL. If the cell density is $3x10^6$ cells/mL and 97% viability, then calculate $3x10^6$ x 97% to obtain the number of viable cells /mL.

Warm media and DMSO to room temperature.

Use 3-5 mL of the 10% DMSO freeze media in a 1:1 mix to the media. Use a 5 mL pipette to mix at least 3 times.

Calculate how many vials, centrifuge tubes and pipettes you will need and expose the items to UV-light for 30 min.

Transfer 6 mL (from calculations in 1) to a centrifuge tube. Centrifuge at 800 rpm for 5 min.

Start labeling the 15 mL centrifuges Nunc tubes.

Set Nucs vials in a tray for convenient handling.

Transfer the tube from the centrifuge and remove the supernatant with the 10 mL pipette.

Add 3.5 mL of the 5% DMSO/ media to the pellet.

Resuspend with a 2 mL pipette and look closely to make sure the whole pellet is solved.

Transfer 1 mL to a Nuc vial.

Place the Nucs inside a Nalgene$^{TM}$ Cryo 1 $^o$C Freezing Container and place in the -70$^o$C freezer overnight.

On the following day prepared with: labcoat, goggles, plastic gloves and Cryogen gloves

transfer the vial from the -70$^o$C freezer to the BioCane dewar with liquid Nitrogen.

## A.8 Loading Cells into the Microfluidic Cell Culturing Device

Microscope and centrifuge is moved to the laminar flow hood, sit for 30 min.

Transfer large Petri dishes with the Plexiglas® covers and PDMS devices to the biological hood for 30 min of UV exposure.

Assemble the device at the laminar flow bench.

Expose the device for another 30 min of UV-light in the biological hood.

Load the device with 96% EtOH for 3 min to fill the channels. Then switch to 50 % EtOH for 3 min and finally rinse the channels with 3 min of ddH2O.

In the experiments using 2% Bovine Serum Albumin (BSA), the BSA was left in the channels for 10 min.

In the experiments using a 2μM Human Fibronectin (HFN), the HFN was left in the channel for 10 min.

While the PDMS is being coated, prepare the cell sample. Transfer 1 mL of cell from a cell culture flask. Mix a 1:1 ratio of cells to Trypan Blue. Use a haemocytometer to determine the cell viability and cell density. Then transfer 2 mL of cells from flask to sterile Eppendorf™ tube, centrifuge the sample for 5 min at 800 rpm. Resuspend the cells in approximately 1 mL of fresh media to reach a seeding density of $1x10^6$ cells/mL.

Load cells to the device by applying a low vacuum flow at one of the reservoirs until all the channels are filled with cells.

Place on the motorized hamster wheel for 2 min and centrifuge at a speed of 60 rpm.

Image the cell loading on the inverted microscope. Reload with additional cells, if needed.

Transport the device to the bio hood. Clean the outer parts of the device using 96% EtOH. Let the ethanol evaporate in the bio hood before placing the device in a new Petri dish with 10 mL double distilled water.

Place the Petri dish inside the incubator set at 37°C with 5% $CO_2$ in air.

# Appendix 4 - References

(1)    Sims, C. E.; Allbritton, N. L. *Lab Chip* **2007**, *7*, 423-440.

(2)    Kim, S. M.; Lee, S. H.; Suh, K. Y. *Lab Chip* **2008**, *8*, 1015-1023.

(3)    Culbertson, C. T.; Jacobson, S. C.; Ramsey, J. M. *Analytical Chemistry* **2000**, *72*, 5814-5819.

(4)    Poole, C. F. The essence of chromatography, Elsevier, Detroit **2003**.

(5)    Hsien, C. H.; Chen, C.; Folch, A. *Lab Chip* **2004**, *4*, 420-424.

(6)    Jorgenson, J. W.; Lukacs, K. D. *Analytical Chemistry* **1981**, *53*, 1298-1302.

(7)    Skoog, D. A.; Holler, F. J.; Nieman, T. A. **1992**.

(8)    Ewing, A. G.; Wallingford, R. A.; Olefirowicz, T. M. *Analytical Chemistry* **1989**, *61*, 292-303.

(9)    L.Copper, C. *Journal of Chemical Education* **1998**, *75*, 343-351.

(10)    Giddings, J. C. Unified Separation Science, John Wiley & Sons, Inc, Canada **1990**.

(11)    Lauffer, M. A. *Journal of Chemical Education* **1981**, *58*, 250-256.

(12)    Rice, C.; Whitehead, R. *J. Phys. Chem* **1965**, *69*, 4017-4024.

(13)    Culbertson, C. T.; Jacobson, S.; Ramsey, J. M. *Talanta* **2002**, *56*, 365-373.

(14)    Sternberg, J. C.; Giddings, J. C.; Keller, R. A. *Advances in Chromatography* **1966**, *2*, 205-270.

(15)    Culbertson, C. T.; Jacobson, S. C.; Ramsey, J. M. *Analytical Chemistry* **1998**, *70*, 2285-2291.

(16)    Heiger, D. N. High Performance Capillary Electrophoresis, Hewlett-Packard: Paris **1992**.

(17)   Giddings, J. C. *Journal of Chromatography* **1961**, *5*, 25-76.

(18)   Culbertson, C. T.; Jacobson, S. C.; Ramsey, J. M. *Analytical Chemistry* **1998**, *70*, 3781-3789.

(19)   Kennedler, E. In High Performance Capillary Electrophoresis: Theory, Technique, and Application, Wiley-Interscience **1998**, 146.

(20)   Dittrich, P. S.; Tachikawa, K.; Manz, A. *Analytical Chemistry* **2006**, *12*, 3887-3908.

(21)   Roman, G. T.; Hlaus, T.; Bass, K. J.; Seelhammer, T. G.; Culbertson, C. T. *Analytical Chemistry* **2005**, *77*, 1414-1422.

(22)   www. invitrogen.com.

(23)   Bruckhalter, J.; Seiwald, R. *USPTO* **1960**, *2,937,186*.

(24)   Attiya, S.; Jemere, A. B.; Thompson, T.; G, F.; Seiler, K.; Chiem, N.; Harrison, D. J. *Electrophoresis* **2001**, *22*, 318-327.

(25)   Davis, J. M. Basic Cell Culture: A Practical Approach, Oxford University Press, USA **2002**.

(26)   Beebe, D.; Folch, A. *Lab Chip* **2005**, *5*, 10-11.

(27)   Freshney, R. I. Culture of Animal Cells, Wiley-Liss, New Jersey **1994**.

(28)   Luzzi, V.; Murtazina, D.; Allbritton, N. L. *Analytical and Biochemistry* **2000**, *277*, 221-227.

(29)   Roman, G. T.; Chen, Y.; Viberg, P.; Culbertson, A. H.; Culbertson, C. T. *Analytical and bioanalytical chemistry*  **2007**, *387*, 9-12.

(30)   Voet, D.; Voet, J. G.; Pratt, C. W. Fundamentals of Biochemistry, John Wiley & Sons, Inc, Dublin **2006**.

(31)   www.library.tedankara.k12.tr.

(32)    Swedler, J. V.; Ariaga, E. A. *Anal. Bioanal Chem* **2007**, *387*, 1-2.

(33)    Carlo, D. D.; Lee, L. P. *Analytical Chemistry* **2006**, *Dec 1*, 7918-7925.

(34)    Luzzi, V.; Lee, C.-L.; Allbritton, N. L. *Analytical Chemistry* **1997**, *69*, 4761-4767.

(35)    Meredith, G. D.; Sims, C. E.; Soughayer, J. S.; Allbritton, N. L. *Nature* **2000**, *18*, 309-312.

(36)    Sims, C. E.; Allbritton, N. L. *Lab Chip* **2007**, *7*, 423-440.

(37)    Jr., J. E. F.; Machleder, E. M. *Science* **1998**, *280*, 895-898.

(38)    Rao, C. V.; Wolf, D. M.; Arkin, A. P. *Nature* **2002**, *420*, 231-238.

(39)    Yu, H.; Meyvantsson, I.; Shkel, I. A.; Beebe, D. J. *Lab Chip* **2005**, *5*, 1089-1095.

(40)    Carlo, D. *Analytical Chemistry* **2006**, 7918.

(41)    Xie, X. S.; Yu, J.; Yang, W. Y. *Science* **2006**, *312*, 228-230.

(42)    Fink, L.; Kwapiszewska, G.; Wilhem, J.; Bohle, R. M. *Exp. Toxicol. Pathol.* **2006**, *57*, 25-29.

(43)    Bodey, B. *Expert Opin. Biol. Ther.* **2002**, *2*, 371-393.

(44)    Borland, L. M.; Kottegoda, S.; Phillips, K. S.; Allbritton, N. L. *Annu. Rev. Anal. Chem* **2008**, *1*, 191-227.

(45)    Cohen, A. A.; Geva-Zatorsky, N.; Eden, E.; Frenkel-Morgenstern, M.; Issaeva, I.; Sigal, A.; Milo, R.; Cohen-Saidon, C.; Liron, Y.; Cohen, L.; Danon, T.; Perzov, N.; Alon, U. *Science* **2008**, *322*, 1511-1516.

(46)    Sims, C. E.; Meredith, G. D.; Krasieva, T. B.; Berns, M. W.; Tromberg, B. J.; Allbritton, N. L. *Analytical Chemistry* **1998**, *70*, 4570-4577.

(47)    Martin, R. S.; Root, P. D.; Spence, D. M. *The Analyst* **2006**, *131*, 1197-1206.

(48)    Gu, W.; Zhu, X.; Futai, N.; Cho, B. S.; Takayama, S. *PNAS* **2004**, *101*, 15861-15866.

(49) Deutsch, M.; Deutsch, A.; Shirihai, O.; Hurevich, I.; Afrimzon, E.; Shafran, Y.; Zurgil, N. *Lab Chip* **2006**, *6*, 995-1000.

(50) Carlo, D. D.; Aghdam, N.; Lee, L. P. *Analytical Chemistry* **2006**, *78*, 4925-4930.

(51) Carlo, D. D.; Wu, L. Y.; Lee, L. P. *Lab Chip* **2006**, *6*, 1445-1449.

(52) Li, P. C. H.; Harrison, J. *Analytical Chemistry* **1997**, *69*, 1564-1568.

(53) Rech, E. L.; Dobson, M. J.; Davey, M. R.; Mulligan, B. J. *Nucleic Acid Res.* **1990**, *18*.

(54) Serpersu, E. H.; Kinosita, K. J.; Tsong, T. Y. *Biochim. Biophys. Acta* **1985**, *812*, 779.

(55) Dower, W. J.; Miller, J. F.; Ragsdale, C. W. *Nucleic Acid Res.* **1988**, *16*, 6127-6145.

(56) Morte, V. J. L.; Karsieva, T. B.; Evans, M. R.; Berns, M. W.; Tromberg, B. *J. Proc. SPIE-Int Soc. Opt. Eng.* **1997**, *2983*, 17-21.

(57) Wheeler, A. R.; Throndset, W. R.; Whelan, R. J.; Leach, A. M.; Zare, R. N.; Liao, Y. H.; Farrell, K.; Manger, I. D.; Daridon, A. *Analytical Chemistry* **2003**, *75*, 3581-3586.

(58) McClain, M. A.; Culbertson, C. T.; Jacobson, S. C.; Allbritton, N. L.; Sims, C. E.; Ramsey, J. M. *Analytical Chemistry* **2003**, *75*, 5646-5655.

(59) Gao, J.; Yin, W.-F.; Fang, Z.-L. *Lab Chip* **2004**, *4*, 47-52.

(60) Hu, S.; Ren, X.; Bachman, M.; Sims, C. E.; Li, G. P.; Allbritton, N. L. *Langmuir* **2004**, *20*, 5569-5574.

(61) Lee, J. N.; Jiang, X.; Ryan, D.; Whitesides, G. M. *Langmuir* **2004**, *20*, 11684-11691.

(62) Hun, Y. S.; Cabrera, L. M.; Song, J. W.; Ftui, N.; Tung, Y.-C.; Smith, G. D.; Takayma, S. *Analytical Chemistry* **2007**, *79*, 1126-1134.

(63) Toepke, M. W.; Beebe, D. J. *Lab Chip* **2006**, *6*, 1484-1486.

(64) Wang, Y.; Lai, H.-H.; Bachman, M.; Sims, C. E.; Li, G. P.; Allbritton, N. L. *Analytical Chemistry* **2005**, *77*, 7539-7546.

(65)    Leibovitz, A. *Am. J. Hyg* **1963**, *78*, 173-183.

(66)    Barth, C. A.; Swartz, L. R. *Proc. Natl. Acad. Sci. U.S.A* **1982**, *79*, 4985-4987.

(67)    Vickers, J. A.; Caulum, M. M.; Henry, C. S. *Analytical Chemistry* **2006**, *78*, 7446-7452.

(68)    Whitesides, S. *Analytical Chemistry* **2003**, *75*, 6544-6554.

(69)    Lee, J. N.; Park, C.; Whitsides, G. M. *Analytical Chemistry* **2003**, *75*, 6544-6554.

(70)    www. gelest.com.

(71)    Walker, G. M.; Ozers, M. M.; Beebe, D. J. *Biomedical Microdevices* **2002**, *4*, 161-166.

(72)    Retting, J. R.; Folch, A. *Analytical Chemistry* **2005**, *77*, 5628-5634.

(73)    Nelson, C. M.; Chen, C. S. *FEBS Letter* **2002**, *514*, 238-242.

(74)    Jacobson, S. C.; Hergenröder, R.; Kounty, L. B.; Ramsey, J. M. *Analytical Chemistry* **1994**, *66*, 2369-2373.

(75)    Meyer, A. R.; Clark, A. M.; Culbertson, C. T. *Lab on a Chip* **2006**, *6*, 1355-1361.

(76)    Culbertson, C. T.; Jorgenson, J. W. *Analytical chemistry* **1994**, *66*, 955-962.

(77)    Scherz, P. Practical Electronics for Inventors, McGraw-Hill **2000**.

(78)    Ashby, D. Electrical Engineering 101, Newnes **2006**.

(79)    Hinshaw, J. V. *LCGC North America* **2004**, *22*, 252-259.

(80)    Weast, R. C.; Astle, M. J. CRC Handbook of Chemistry and Physics **1980**, 61st Ed.

(81)    Culbertson, C. T.; Jacobson, S. C.; Ramsey, J. M. *Talanta* **2002**, *56*, 365-373.

(82)    Meyer, A. R. *Lab on a Chip* **2006**, *6*, 1355-1361.

(83)    Balagadde, F. K.; You, L.; Hansen, C. L.; Arnold, F. H.; Quake, S. R. *Science* **2005**, *309*, 137-140.

(84)    Marcus, J. S.; Anderson, W. F.; Quake, S. R. *Analytical Chemistry* **2006**, *78*, 956-958.